

ESD-TR-68-360

## ESD ACCESSION LIST

ESTI Call No. 65093  
Copy No. 1 of 1 cys.

ESLE

## ESD RECORD COPY

RETURN TO  
SCIENTIFIC & TECHNICAL INFORMATION DIVISION  
(ESTI), BUILDING 1211

Technical Note

1968-38

Experimental Study  
of the  
Low Frequency Operation  
of a Cassegrainian Antenna

F. I. Sheftman

10 December 1968

Prepared under Electronic Systems Division Contract AF 19(628)-5167 by

**Lincoln Laboratory**

MASSACHUSETTS INSTITUTE OF TECHNOLOGY

Lexington, Massachusetts



AD686065

The work reported in this document was performed at Lincoln Laboratory,  
a center for research operated by Massachusetts Institute of Technology,  
with the support of the U.S. Air Force under Contract AF 19(628)-5167.

This report may be reproduced to satisfy needs of U.S. Government agencies.

This document has been approved for public release and sale;  
its distribution is unlimited.

MASSACHUSETTS INSTITUTE OF TECHNOLOGY  
LINCOLN LABORATORY

EXPERIMENTAL STUDY  
OF THE LOW FREQUENCY OPERATION  
OF A CASSEGRAINIAN ANTENNA

*F. I. SHEFTMAN*

*Group 46*

TECHNICAL NOTE 1968-38

10 DECEMBER 1968

This document has been approved for public release and sale;  
its distribution is unlimited.

LEXINGTON

MASSACHUSETTS

## ABSTRACT

The maximum allowable magnification factor of a conventional Cassegrainian antenna is shown to depend on the subreflector size in terms of wavelength. Use of excessively high magnification leads to inefficient operation, unless special precautions are taken. It is demonstrated experimentally that, for a given subreflector, satisfactory results can be obtained with a variety of feed horn sizes and locations, provided the subreflector can be defocused a distance of up to a few wavelengths. It is further shown that the subreflector shape is not critical if sufficient room is available for compensatory defocusing. Efficient operation is also possible without subreflector defocusing in a near-field configuration involving a large feed horn placed close to a subreflector having high magnification. The three-reflector system, which uses a small dish as the feed aperture, can be operated with little or no subreflector defocusing, but the system has low efficiency due to the low efficiency of the small dish.

Accepted for the Air Force  
Franklin C. Hudson  
Chief, Lincoln Laboratory Office

## CONTENTS

Abstract	iii
I. Introduction	1
II. Horn Feeds	3
III. Focused-Aperture Feeds	10
IV. Conclusions	12
Appendix A – Low Frequency Limit of Cassegrainian Geometry	15
Appendix B – Beam Efficiency	17

## EXPERIMENTAL STUDY OF THE LOW FREQUENCY OPERATION OF A CASSEGRAINIAN ANTENNA

### 1. INTRODUCTION

#### A. Description of the Problem

The microwave Cassegrainian antenna is derived from the optical Cassegrainian telescope and presents no special problems at relatively short wavelengths. Almost any convenient point between the main dish and its focal point may be chosen as the feed location. This flexibility disappears at lower frequencies when the wavelength is no longer sufficiently small with respect to the subreflector. In that case, the ray-optics approximations are not valid, and the Cassegrainian geometry must conform to certain restrictions in order to achieve efficient operation.

The point at which the wavelength begins to be a problem is not sharply defined. It is possible to obtain a qualitative estimate by considering the Cassegrainian system of Fig. 1 in its receiving mode. The basic geometric requirement is that the hyperbolic subreflector bring the radiation incident upon it from the main reflector to a "point" focus at the feed location  $P_1$ .

In reality, the field in the focal region at  $P_1$  has a finite space distribution<sup>1</sup> that is a function of the subreflector size and the wavelength. In optics this distribution has often been called the Airy disc or the focal "spot." Its minimum diameter is given approximately by the diffraction formula

$$S \approx \frac{2.4\lambda}{d} R$$

where

$S$  = 10-dB diameter of focal spot

$d$  = diameter of subreflector

$R$  = distance of focus from subreflector

$\lambda$  = wavelength

The formula applies to apertures that are large in terms of wavelength, and it holds equally well for focal regions, near-field radiation, or far-field radiation.<sup>2</sup> The assumption is made that the aperture illumination has a typical taper and is properly phased (focused) for the particular distance of operation. It can be seen that  $S/R$ , the angular width of the "spot," is independent of  $R$ .

A few instructive examples of the limitations imposed by diffraction are given in Table 1. Except in the third case, the "spot" sizes are sufficiently small\* to be suitable for a conventional

\* Examination of Appendix A will show that for  $S/d < 1/4.2 = 0.238$  the "spot" is sufficiently small. It should be remembered, however, that these values become approximate when  $d/\lambda$  is not large. A value of 10 may not be sufficiently large.<sup>3,4</sup>

TABLE I  
LIMITATIONS IMPOSED BY DIFFRACTION  
FOR CONVENTIONAL CASSEGRAINIAN SYSTEM

$d/\lambda$	$R/d$	$S/d$
100	5	0.105
100	1	0.021
10	5	1.05
10	1	0.21

Cassegrainian system, which utilizes a small feed with a uniform phase distribution across its aperture. In practice, such a small feed is equivalent to a directive point source.

In the third example, the "spot" diameter is equal to the diameter of the subreflector, and the geometrical requirement of a "point" focus is not met. This does not necessarily imply that a large "spot" is unusable. Indeed, it would seem that a large feed with suitable amplitude and phase distributions may be designed to match the distributions of the large "spot."

Additional insight into the required aperture distributions of the large feed may be obtained by considering the Cassegrainian system of Fig. 1 in its transmitting mode. If the illumination incident on a hyperbolic subreflector appears as a spherical wave originating at  $P_1$ , satisfactory operation will result regardless of the size or location of the source.

#### B. Purpose and Scope of Study

This study grew out of an investigation of the operation of the Haystack antenna at L-band. Since the predominant use of the Haystack antenna was expected to be in the high frequency bands, a large magnification factor was originally chosen, so that the feed point would be near the vertex of the main reflector. At L-band, this geometry requires a feed aperture comparable in size to the subreflector. The purpose of this study is to investigate the performance of this system, which violates restrictions derived in Appendix A for a conventional Cassegrainian system.

Of course, choice of a small magnification factor would have solved the illumination problem at the price of locating the feed near the subreflector, as has been done, for example, by the Jet Propulsion Laboratory.<sup>5</sup> This can be, however, an inconvenient and inaccessible location for a system in which quick change of feed assembly and accessory equipment is necessary. A change in subreflector size was ruled out for Haystack.

Two general types of feeds are considered. The first is the conventional horn; the second is the focused-aperture feed, an example of which is the three-reflector system.<sup>6</sup> It employs a small parabolic reflector (illuminated by a primary feed) as the Cassegrainian feed aperture at  $P_1$  (Fig. 1). Focusing of the primary feed produces a suitable phase distribution across the aperture at  $P_1$ . In theory, a horn-lens combination can also be used as a focused-aperture feed.

At L-band the large size of the conventional horn aperture resulted in its operation in the region intermediate between the far field and the near field. Both the far-field and near-field Cassegrainian<sup>7</sup> systems are straightforward in their operation. But the intermediate region, of interest here, is complex and difficult to analyze. Also, little information was available on the phase characteristics of the focused aperture feed. Consequently, an experimental approach to the problem appeared desirable.

### C. The Experimental Procedure

The experimental work was performed at a frequency of 28.4 Ge/s on a 1/20 scale model of the Haystack antenna.\* Most of the measurements were carried out at the Lincoln Laboratory 2000-foot ground-reflection range. First, the phase and radiation patterns of some of the feeds were measured at a distance equal to the subreflector distance. The far-field patterns and gain were also taken for comparison purposes and as a check on the feed efficiency. Then the feeds were installed in the Cassegrainian system and evaluated.

The main reflector was a 6-foot precision dish. Provision was made for adequate axial movement of the subreflector and the feed. Each was coupled to a synchro which was connected to a pattern recorder. This permitted rapid and convenient recording of focusing curves, as well as of radiation patterns. The gain of the system was measured by comparison with a standard gain horn mounted at the side of the 6-foot dish. Permanent waveguide plumbing was installed for this purpose, with an E-H tuner in the dish line and also in the horn line. A waveguide switch permitted rapid gain comparison.

An additional check on the secondary gain measurement was made with several feeds known from experiment to be reasonably efficient. One was a small horn in a conventional far-field Cassegrainian geometry, which required a special subreflector with a magnification factor of 3. Another test involved the Keppel feed,<sup>8</sup> a limiting case of the Cassegrainian geometry. Since much of the waveguide plumbing was common to all feeds, their relative gain could be determined with high confidence. The estimated accuracy of the relative measurements was about  $\pm 0.3$  dB.

## II. HORN FEEDS

### A. The Three Regions of Operation

In the far field typical horns have an angular field distribution that is invariant with distance. The phase center of the radiation is located at, or near, the aperture. No difficulty is experienced in using an antenna in this region; that is, beyond the distance given approximately by

$$R = \frac{2A^2}{\lambda} .$$

In fact, for some applications, operation at half this distance is satisfactory.

For distances smaller than the approximate value given by  $R/8$  the radiating near field is well established. There, the amplitude and phase resemble closely the aperture distribution. This regular behavior is exploited to good advantage in the near-field Cassegrainian system.<sup>7</sup>

For distances between the approximate boundaries of the far field and the near field, the amplitude of the radiation field varies with distance in a complex manner. The phase center of a typical horn moves increasingly behind the aperture as the distance is decreased.<sup>9</sup> It is in this region that a feed horn is most troublesome and difficult to utilize efficiently.

### B. The Large Horn

To determine the behavior of the experimental Cassegrainian geometry when fed by simple rectangular horns, a large horn was constructed and then reduced in size in small steps.

---

\* This corresponds to L-band operation on the full-scale antenna.

Initially, both subreflector and horn were placed in their nominal positions. Then, the horn was moved axially for maximum secondary gain. Next, the subreflector was focused for maximum gain. These adjustments were alternated until both subreflector and horn converged to their optimum positions. As the horn aperture was reduced, the optimization process was repeated for each dimension.

The original horn aperture was  $7.65 \times 10.68\lambda$ , which is much greater than the low frequency limiting figure\* given by

$$A < d/4.2 = \frac{13.45\lambda}{4.2} = 3.2\lambda$$

This large aperture was chosen because its diagonal dimension was equal to the subreflector diameter. The horn was long enough ( $90\lambda$ ), so that its maximum intrinsic phase error was about  $0.16\lambda$ .

The measured primary radiation patterns of the original horn are given in Fig. 2 for the far field as well as for the intermediate region.<sup>†</sup> The beam broadening and the resulting increased spillover are evident at the shorter distance. The relative phase (measured in the intermediate region only) indicates the deviation from a spherical phase front. Thus, a straight line represents a perfectly circular phase front centered at the horn aperture. For comparison, the phase front of a plane wave is shown on the same chart. The measured relative phase of the horn may be considered approximately circular, but with a center some distance behind the aperture. The phase was measured with the aid of the simple setup shown in Fig. 3. The assumption that the small reference horn radiates a spherical wave centered at its aperture is basic for the accuracy of this method.

The measured far-field gain of the large horn was 28.6 dB, which is about 1/3 dB less than the value calculated by the method described in NRL Report 4433 (Ref. 10). It will be assumed that the gain loss is due to waveguide attenuation. With aid of the formula derived in Appendix B, the 10-dB beam efficiency can be calculated:

$$\begin{aligned} \eta_b &= 8.16 \times 10^{-6} G_o (W_{10})^2 \\ &= 8.16 \times 10^{-6} (726) (11.25)^2 = 0.75 \end{aligned}$$

Thus, about 75 percent of the total radiated power is concentrated in the upper 10-dB portion of the main beam. If the calculated gain of the horn is used, the beam efficiency becomes 81 percent.

The measured gain of the large horn at the distance of  $60\lambda$  was 1.5 dB lower than the far-field value. Since the beam shape is distorted, particularly in the H-plane, the above formula for beam efficiency is not applicable here. Qualitatively, it can be seen that the greater beam-width in the near field accounts to some extent for the lower gain, so the beam efficiency is not quite 1.5 dB lower. In addition, the phase error of the horn radiation, if uncorrected, would become a phase error across the main dish and further decrease the secondary gain.

When the large horn was installed in the Cassegrainian system of Fig. 1, maximum gain was obtained with the hyperbolic subreflector displaced  $0.35\lambda$  toward the main dish and the horn

---

\* See Appendix A.

† Unless otherwise indicated, all figures present measured data.

aperture located  $25\lambda$  forward of  $P_1$ . The horn-to-subreflector distance was  $30\lambda$ . The resulting patterns are shown in Fig. 4, other details being summarized in Table I. The measured gain was 51.2 dB. If allowance is made for the estimated 1/3 dB attenuation loss of the horn, the gain becomes 51.5 dB, or 0.6 dB below 52.1 dB, the value representing 55 percent aperture efficiency. From the formula of Appendix B, the corrected secondary 10-dB beam efficiency can be determined:

$$\begin{aligned}\eta_b &= 8.16 \times 10^{-6} G_o (W_{10})^2 \\ &\approx 8.16 \times 10^{-6} (1.41 \times 10^5) (0.67) (0.71) = 0.547\end{aligned}$$

where the geometric mean of the somewhat unequal beamwidths is used. This beam efficiency is lower than the 61 percent figure given in Appendix B for a typical dish.

To determine the importance of defocusing the subreflector, it was next placed in its correct design position, and only the feed horn was moved for maximum gain. The best gain obtainable under this condition was about 1/2 dB lower than before. The horn was  $24\lambda$  away from the subreflector. The additional aperture blockage due to this forward horn position was responsible only in small part for the gain loss. The patterns were not simultaneously well focused in both planes, the E-plane pattern having 14-dB shoulders. When both subreflector and horn were placed in their design positions, the corrected secondary gain was 50.5 dB, or 1.0 dB down from the optimum case.

Use of a parabolic subreflector, instead of the hyperbolic one, produced 0.3 dB more gain. The subreflector-to-horn spacing was about  $27\lambda$ . The subreflector itself was defocused about  $\lambda/2$  away from the main dish. The secondary patterns had somewhat higher close-in sidelobes, and the beamwidth was smaller. After allowance was made for this, the secondary beam efficiency was found to be actually somewhat lower than with the hyperbolic subreflector.

The gain of the system was not very sensitive to horn position except for a small ripple of approximately  $\pm 0.4$  dB [Fig. 5(a)]. Since the maxima (or minima) were separated by  $\lambda/2$ , this was assumed to be an interaction phenomenon between the closely spaced horn and subreflector. The fluctuation could be changed in amplitude, but it could not be eliminated by an E-H tuner placed at the throat of the horn. The beamwidth and sidelobes exhibited substantial changes when the horn was moved from a maximum to a minimum. No change was noted, however, when the horn was moved from one maximum to other nearby maxima, or from one minimum to other nearby minima. Thus, small changes in the horn position had a greater effect than large changes, provided the latter were in multiples of  $\lambda/2$ . Due to the relatively long distance between the horn and the subreflector, this behavior would tend to produce a frequency dependence of both gain and patterns.

### C. Smaller Horns

As the horn aperture was reduced, the subreflector defocus was reduced and then reversed. The feed at first moved closer to  $P_1$ , then gradually came back toward the subreflector. The gain fluctuation with horn position decreased in amplitude as the horn moved farther away from the subreflector and as the horn was reduced in size, provided the E-H tuner was properly tuned. A summary of the measured results is given in the first group of Table II, where all the entries are maximum gain cases. The defocus of the hyperbolic subreflector is considered positive when

TABLE II  
MEASURED CASSEGRAINIAN PERFORMANCE WITH HORN FEEDS (M = 10.75)

Entry Number	Horn Aperture Size ( $\lambda$ )				Calculated Far-Field Distance ( $\lambda$ )				Horn-to-Subreflector Distance ( $\lambda$ )		Subreflector Defocus ( $\lambda$ )		Calculated 10-dB Horn Beamwidth (deg)		Spillover Angle (deg)		Secondary Beamwidth (deg)		Secondary Sidelobe Level (dB)		Relative Secondary Gain (dB)		
	EP		HP		EP		HP		EP		HP		EP		HP		EP		HP		EP		
1	7.65	10.68	11.7	22.8	30	-0.35	11.5	11.2	24.0	0.67	0.71	24.5	27								-0.6		
2	7.12	9.93	10.1	19.7	30	-0.30	12.4	12.1	24.0	0.69	0.72	22.5	21								-0.5		
3	6.52	9.12	8.5	16.6	46.5	0	13.5	13.2	15.8	0.69	0.67	25	23.5								-1.1		
4	5.93	8.33	7.0	13.9	42	+0.01	14.8	14.4	17.5	0.68	0.68	23	24.5								-0.6		
5	5.36	7.55	5.7	11.4	41	+0.05	16.4	15.9	17.8	0.67	0.67	22.5	22								-0.5		
6	4.78	6.72	4.6	9.0	35	+0.05	18.4	17.9	20.6	0.67	0.67	21.5	24.5								-0.5		
7	4.18	5.88	3.5	6.9	33	+0.05	21.0	20.4	21.7	0.65	0.65	20	20								-0.5		
8	3.61	5.13	2.6	5.3	28	+0.36	24.4	23.4	25.5	0.64	0.64	21	20.5								-0.1		
9	3.22	4.64	2.1	4.3	23	+0.58	27.3	25.9	30.1	0.64	0.64	21	21								+0.2		
10	2.64	3.82	1.4	2.9	20.6	+0.75	33.4	31.4	33.2	0.64	0.62	21	21.5								+0.1		
11	2.31	3.45	1.1	2.0	16.6	+0.97	38.4	38.1	40	0.63	0.63	22	21.5								+0.17		
12	2.31	3.45	1.1	2.0	13	+1.27	38.4	38.1	48.5	0.66	0.66	23.5	22.5								0		
13	2.31	3.45	1.1	2.0	11	+1.66	38.4	38.1	55	0.68	0.68	24.5	23.5								+0.1		
14	1.92	2.64	7.4	14	11.1	+1.66	45.8	45.5	55	0.63	0.63	22.5	21.5								+0.1		
15	1.35	1.85	3.6	6.9	9.1	+1.73	65.2	65	63	0.62	0.63	21.5	21.5								-0.57		

the displacement is away from the main reflector. The calculated 10-dB beamwidth of the horns is the far-field value; the spillover angle is the angle intercepted by the hyperbolic subreflector at the feed aperture. The relative secondary gain is the amount the measured gain exceeds the value representing 55 percent aperture efficiency. Allowance was made for the estimated horn attenuation loss of about 1/3 dB for the first group. Also, for this group of horns the wall thickness was  $0.6\lambda$ .

The other horns had a reasonable wall thickness and were believed to have no significant losses. The data show that the gain increases when the horn size permits operation at a distance approaching the far-field region. It is interesting that the subreflector can be focused even when the feed is brought very close to it. The secondary radiation patterns for some of the horns are given in Figs. 6 through 8. The insensitivity of the gain to horn displacement is illustrated in Fig. 5(a) for a number of horns. Of course, the gain was quite sensitive to subreflector position for all horn sizes, as can be seen in Fig. 5(b), where the greatly expanded scale of the abscissa should be noted. The half-wave periodicity is less apparent, but it can still be identified in these curves. The relative position along the abscissa or the ordinate of all curves is arbitrary in both parts of the figure.

For any subreflector position there is a corresponding feed horn position that produces maximum relative gain. In fact, there is a reasonably broad range of subreflector positions and the corresponding best horn positions that produce gains quite close to the optimum gain, as well as good patterns. An example of this is provided by the second group of data in Table II (entry numbers 11 through 13). There seems to be little difference in the gain of the first and third entries, yet the latter is unquestionably superior. Consideration of the secondary 10-dB beam efficiencies will make this clear. The first entry in the  $2.31 \times 3.15\lambda$  group has an efficiency

$$\eta_b = 8.16 \times 10^{-6} (1.69 \times 10^5) (0.63)^2 = 0.547 .$$

The third entry has an efficiency

$$\eta_b = 8.16 \times 10^{-6} (1.66 \times 10^5) (0.68)^2 = 0.627 .$$

Thus the lower beam efficiency implies more power lost in the sidelobes. Examination of the geometry, as given in Table II, shows that the greater separation between the horn and the subreflector does indeed cause increased spillover losses, as well as the higher edge illumination that leads to narrower secondary beamwidth. For a low noise antenna, the highest gain-beamwidth product (or beam efficiency) is desired, rather than merely the highest gain.

#### D. Effect of Horn Phase Error

All the previous measurements were made with feed horns having low aperture phase error. In the case of the larger horns, this involved great axial length. If the length is reduced substantially, the intrinsic phase error of the horn increases, producing wider primary patterns, higher sidelobes, and lower gain. These effects are similar to those caused by phase error due to near-field operation. In either case, the system performance of a Cassegrainian antenna would be degraded, unless proper precautions are taken.

Two feed horns with substantial phase error were tested. The first horn had an aperture of about  $5 \times 7\lambda$  and the rather short axial length of  $17.5\lambda$ . This produced a phase error of  $0.3\lambda$  in the H-plane and  $0.16\lambda$  in the E-plane. After installation in the system (Fig. 1), the horn and the

subreflector were adjusted for maximum gain. The resulting patterns of Fig. 9 can be compared with the patterns of Fig. 5, which are for a horn of nearly equal aperture but with low phase error due to its greater length. The secondary patterns in the E- and H-planes are not simultaneously well focused in the case of the short horn. This is to be expected, since the E- and H-plane flare angles are quite unequal. The secondary gain with this horn was compared with the gain produced by the longer horn (Table II) and found to be equal within experimental accuracy.

The short horn was only  $19.5\lambda$  away from the subreflector, which is nearly half the distance of  $35\lambda$  shown in Table II for the longer horn. The subreflector position was not significantly different, so it seems reasonable to conclude that the phase center of the short horn was also about  $35\lambda$  away. This is consistent with the general results of Ref. 9, where it is shown that the phase error and the violation of the far-field condition tend to move the phase center to the rear of the aperture.

The second horn was tried in a near-field configuration proposed by RCA.<sup>11</sup> Unlike the near-field Cassegrainian antenna described in Ref. 7, where a parabolic subreflector is required, the RCA approach calls for a hyperbolic subreflector. The basic assumption is that the phase center of a sufficiently flared horn is at its apex, provided near-field conditions are satisfied. Consequently, if the apex of the horn is placed at the remote focal point of the hyperbolic subreflector, the basic phase requirement will be met. The horn flare angle and its length will then determine the illumination taper.

RCA used a square multi-mode horn in order to establish symmetry of illumination in the E- and H-planes. Since only a dominant-mode square horn of suitable size was available, it was felt that useful comparison data could be obtained with it at a considerable saving in time despite the different distributions in the principal planes.

The horn aperture was  $7.2\lambda$  square, and its axial length about  $29\lambda$ , resulting in a phase error of about  $0.54\lambda$ . It was installed in the Cassegrainian antenna and adjusted, as was the subreflector, for maximum gain. The horn-to-subreflector separation turned out to be  $19\lambda$ , or  $0.36\lambda^2/\lambda$ , which is close to the near-field distance. The secondary patterns are shown in Fig. 10, where the greater beamwidth in the H-plane is noticeable. This is due to near-field operation, which causes the subreflector illumination, and consequently the main dish illumination, to resemble the horn aperture distribution. The measured secondary gain was 52.1 dB (55 percent efficiency) within experimental error. The subreflector was essentially in its correct position, but the horn apex was displaced about  $4.8\lambda$  closer to the subreflector than expected. Use of a multi-mode horn should improve the secondary gain.

#### E. Gain Calibration

The performance of the Cassegrainian system with a subreflector magnification factor and a feed size within the restrictions derived in Appendix A was expected to provide a useful check on the measurements. Accordingly, a subreflector with a magnification of 3 and a feed horn with an aperture of  $1.92 \times 2.64\lambda$  were installed. After both were adjusted for maximum gain, the secondary patterns of Fig. 11 were obtained. Comparison with the patterns of Fig. 7, obtained with the subreflector having  $M = 10.75$ , shows significant differences in beamwidth. Since the secondary gain was very close to 52.1 dB (55 percent efficiency) in either case, the wider patterns of Fig. 11 are clearly preferable, as was demonstrated earlier for the  $2.31 \times 3.15\lambda$  horn.

When the horn and subreflector ( $M = 3$ ) were placed in their design positions, the gain was reduced by about 0.7 dB. The patterns became nearly identical in the principal planes, assuming

the expected beamwidths ( $W_{10} = 0.68^\circ$ ). As in the case of the subreflector with the higher magnification, there was a substantial range of subreflector positions, for each of which the feed could be adjusted for a maximum relative gain not appreciably below the optimum value. Other data indicated that equality of beamwidths was probable at some of these positions. Since the feed horn had low phase error, no explanation for the lower gain at the design positions is available. It is another demonstration of the desirability of a wide range of focusing adjustment. The focal point of the main dish was determined from measurements with small focal-plane waveguide feeds.

The results with the two different hyperbolic subreflectors show that the subreflector shape is not very critical, provided there is no restriction on the amount of focusing. This conclusion is reinforced by the performance of a parabolic subreflector ( $f = 2.24$  inches), which was substituted for the hyperbolic subreflectors. The best gain was only a few tenths of a dB lower, and the patterns were intermediate in width when compared with those produced by the two preceding hyperboloids.

A more detailed examination of the far-field Cassegrainian geometry established with the hyperbolic subreflector having the magnification factor of 3 will be enlightening. There are no near-field complications and the feed horn characteristics can be determined in a straightforward manner. Figure 12 shows the far-field primary patterns of the  $1.92 \times 2.64\lambda$  horn. In the optimum case the subreflector intercepted an angle of  $53^\circ$ , giving a subreflector edge illumination of about  $-15$  dB. In the design positions, the edge illumination was  $-10$  dB. The measured gain of the horn was  $17.12$  dB, which is  $0.34$  dB higher than the figure calculated by the method described in NRL Report 4433 (Ref. 10). The discrepancy is reasonable in view of the fact that the method loses accuracy for smaller horns.

The calculated beam efficiency of the small horn down to the  $53^\circ$  width is 0.90. Thus 90 percent of the total radiated power is incident on the subreflector. The calculated 10-dB beam efficiency is 0.86, which is 5 percent higher than the figure calculated earlier for the large horn.

It is interesting to note that the 90 percent feed horn beam efficiency produces a secondary aperture efficiency of only 55 percent. A more important figure of merit is the secondary 10-dB beam efficiency

$$\eta_b = 8.16 \times 10^{-6} (0.162 \times 10^6) (0.68) (0.70) = 0.63$$

Thus,  $0.63/0.90 \approx 0.7$  of the power incident on the subreflector is radiated in the upper 10-dB portion of the main beam.

One limiting case of the Cassegrainian geometry involves the use of a flat subreflector and a very small horn placed close to it. Keeping<sup>8</sup> showed that this is a reasonably efficient feed. With a circular unflared waveguide feed  $0.85\lambda$  in diameter and a flat reflector  $14.4\lambda$  in diameter, an aperture efficiency of 55 percent was indeed attained. The gain did not change perceptibly when a  $0.96\lambda$  horn was substituted. The patterns were similar to those obtained with the curved subreflectors and larger feed horns. Since much of the waveguide plumbing was common to most feed systems, a reliable relative gain figure was obtained in each case, regardless of the absolute accuracy of the 55 percent aperture efficiency figure.

A third check of the secondary gain was made by placing the  $0.85\lambda$  circular horn at the focus of the 6-foot dish. The best gain with this non-Cassegrainian arrangement was 0.3 dB below the 55 percent efficiency level. In this case, however, the waveguide plumbing was different, so the result is useful only as an approximate check.

### III. FOCUSED-APERTURE FEEDS

#### A. Near-Field Measurements of $13.5\lambda$ Dish with Clavin Feed

A three-reflector system with a  $13.5\lambda$  dish as the Cassegrainian feed aperture was assembled. The small dish was placed at  $P_1$  (Fig. 1), and the phase across its aperture was adjusted by focusing the primary feed. This was expected to eliminate the spillover problem and hopefully generate a subreflector illumination that appears to have a phase center at  $P_1$ .

The  $f/d$  ratio of the  $13.5\lambda$  dish was 0.22, which was small enough to minimize primary feed spillover. The size of the dish and the  $60\lambda$  distance to the subreflector led to operation at  $d^2/3\lambda$ , which nearly satisfied the near-field condition. To illuminate the dish, a Clavin feed<sup>6,12</sup> was first tried. Due to the small size of this feed at the test frequency of 28.4 Gc/s, it was difficult to measure the primary patterns with any degree of reliability. Therefore, the feed parameters were adjusted for best results after the feed was installed in the small dish. The feed was matched to a VSWR of about 1.5:1 by adjusting the dipole length and the position of the short inside the waveguide (Fig. 13). Reasonably good phase and amplitude patterns were obtained when the Clavin feed was focused for maximum gain. Figure 13 shows the patterns and phase of the  $13.5\lambda$  dish at the distance of  $60\lambda$ . The main beam is well shaped and symmetrical. The subreflector edge illumination at  $-14.5$  dB is somewhat low, but should not affect seriously the system efficiency. Strictly speaking, the usual criterion of near-field operation is not relevant in the case of a focused aperture. The focusing causes the far-field behavior to occur at the near-field distance. The measured phase indicates that the dish radiates a nearly spherical wave centered at  $P_1$  rather than a plane wave.

The gain at the distance of  $60\lambda$  was measured with a small standard gain horn having low phase error. The measured figure of 27.6 dB represents a rather low aperture efficiency for the  $13.5\lambda$  dish, but this is not significant in the present application. The more important criterion of beam efficiency should be considered. The calculated 14.5-dB beam efficiency is approximately 0.61. This ratio is much lower than the 90 percent figure obtained previously in the case of the small horn. From the ratio 0.61/0.90, it is seen that a gain loss of about 1.7 dB should occur when the small dish is used as a feed in the Cassegrainian system.

#### B. Far-Field Measurements of $13.5\lambda$ Dish with Clavin Feed

Since little published information was available on the reliability of near-field measurements, some far-field tests were conducted at a distance of 2000 feet on the  $13.5\lambda$  dish. The Clavin feed was focused for maximum gain, producing the patterns of Fig. 14. The feed position in this case was  $0.36\lambda$  closer to the dish than in the near field. This compares favorably with the curves given by Cheng and Moseley,<sup>2</sup> but it does not agree with the ellipsoidal-reflector approach of Cheng.<sup>13\*</sup>

The measured far-field gain of 27.0 dB was 0.6 dB lower than the near-field value. The 10-dB beamwidth is somewhat greater than at the smaller distance and the patterns are slightly distorted.

\* The disagreement is due to the nature of the approximation made by Cheng. His result is valid only for dishes having rather large  $f/d$  ratios. If the ellipse that is a best fit to the  $13.5\lambda$  dish (focused at  $60\lambda$ ) is found by other methods, the short focal length of the ellipse does indeed give the exact defocus measured above.

### C. Performance of the Cassegrainian Antenna with the $13.5\text{-}\lambda$ Dish and Clavin Feed

The  $13.5\text{-}\lambda$  dish with the Clavin feed was next installed in the Cassegrainian geometry of Fig. 1. Both the subreflector and the Clavin feed were focused, in turn, for maximum gain. The position of the small dish was not critical. The radiation patterns of the main dish are shown in Fig. 15 for the optimum case. Some asymmetry is noticeable, and the H-plane pattern does not appear to be well focused. The measured gain was 1.5 dB below the value representing 55 percent efficiency, which is close to the 1.7-dB figure predicted from the near-field measurements. The calculated 10-dB beam efficiency of the main dish is 0.447. The ratio  $0.447/0.61$  shows that about 73 percent of the power incident on the subreflector is radiated in the upper 10-dB portion of the beam.

The above results were obtained when the Clavin feed was essentially in the near-field position. The hyperbolic subreflector was also reasonably close to its design position, being displaced toward the main dish by less than  $\lambda/5$ . A variety of pattern widths and sidelobe levels could be obtained with different feed and subreflector positions. Some of the patterns had considerably lower sidelobes at the cost of some loss in gain and somewhat wider beams. The parameters of the Clavin feed could also be changed to improve the main dish patterns somewhat, despite the fact that the same changes tended to produce some deterioration in the near-field patterns. The main dish cross polarization was asymmetrical, but it was at least 25 dB down at the highest points in the diagonal planes.

To see what effect the diameter of the small dish had on the performance of the system, an  $11\text{-}\lambda$  dish with an  $f/d$  ratio of 0.27 was tested with the same Clavin feed. The patterns of the smaller dish were somewhat broader than those of the  $13.5\text{-}\lambda$  dish, but they can be considered equal for all practical purposes. The gain was essentially identical, exhibiting the same drop in value in the far field. The main dish patterns and gain were also comparable with those produced by the  $13.5\text{-}\lambda$  dish. Smaller dishes were not tried, since it was felt that spillover would become important. A  $13.5\text{-}\lambda$  dish with a shorter focal length than the first dish produced lower overall gain.

Higher system gain was obtained with the  $13.5\text{-}\lambda$  dish when several larger subreflectors with different focal lengths and magnifications were tried. The focal lengths of these subreflectors did not seem to be very important, provided they were focused for maximum gain. The larger diameter, however, seemed to be a key to the increase in gain. This improvement was accompanied by a narrower main dish beam and higher sidelobes. A simple calculation showed that the beam efficiency of the main dish was essentially the same in all cases. Evidently, the feed efficiency was of basic importance.

The above results once again illustrate the lack of importance of the precise shape of the subreflector, so long as sufficient focusing is permitted. In the case of the various hyperbolic subreflectors, the Clavin feed was usually close to the near-field position. With a  $19\text{-}\lambda$  parabolic subreflector, the Clavin feed was close to the far-field position.

### D. Limitations of the $13.5\text{-}\lambda$ Dish and the Clavin Feed

Considerable difficulty was experienced with the Clavin feed due to its small size at the test frequency of 28.4 Gc/s. The various parameters of this complex feed were sensitive to small dimensional variations. Moreover, the feed did not seem to have an identical phase center in

the principal planes. This meant that defocusing was a compromise between correcting phase error due to near-field operation and minimizing phase error due to the electrical asymmetry of the feed.

There was no direct method for testing the efficiency of the Clavin feed itself. In an attempt to evaluate the Clavin feed by comparison, a circular waveguide feed  $0.96\lambda$  in diameter was installed in the  $13.5\lambda$  dish. The near-field patterns with this feed were quite good (Fig. 16), and the phase was even better than with the Clavin feed. The far-field patterns, however, were quite unequal in width (Fig. 17). The measured far-field gain was higher than the far-field gain with the Clavin feed. Yet, when the dish and circular feed were installed in the Cassegrainian geometry of Fig. 1, the main dish gain and patterns were comparable to those obtained with the Clavin feed. The calculated 10-dB beam efficiency was 45 percent, and the aperture efficiency was 39 percent.

No near-field gain measurement was made with the circular horn feed and the  $13.5\lambda$  dish. But other near-field measurements showed unexpected behavior. For example, it was found that the H-plane beamwidth of the small dish was almost independent of the feed horn size, while the E-plane width behaved properly. Also, the beamwidth varied as a function of frequency in the H-plane, while the E-plane width remained essentially constant, as it should. At first, the surface tolerance of the  $13.5\lambda$  dish was suspected, but a careful measurement showed it was very accurate. Other considerations finally led to the hypothesis that either the dish diameter or the focal length was simply too small in terms of wavelength.

To investigate this problem, both feeds were installed in an available  $19\lambda$  dish having an  $f/d$  ratio of 0.25. Reasonable behavior was observed in the near field as well as in the far field (Figs. 18 through 21). The measured far-field gain with these feeds was nearly the same, the Clavin feed being approximately 0.3 dB lower. The 10-dB beam efficiency of the  $19\lambda$  dish with the circular horn feed was about 71 percent, while the Clavin feed gave about 67 percent. From these data it was concluded that the Clavin feed is reasonably efficient, provided the dish diameter (or focal length) is not too small. Also, since the small circular feed horn is much more broadband, it was considered preferable to the Clavin feed. Unfortunately, the  $19\lambda$  dish was too directive for use in the geometry of Fig. 1.

#### IV. CONCLUSIONS

Straightforward consideration of the illumination requirements showed that the maximum allowable magnification factor of a conventional Cassegrainian antenna is proportional to the subreflector size in terms of wavelength. At low frequencies, small magnification must be used in order to achieve reasonable efficiency. This implies a relatively small feed located rather close to the subreflector.

In the case of a very broadband Cassegrainian system, where it is desired to have a large magnification factor at high frequencies, efficient operation at low frequencies is still possible without changing the subreflector. Of several available methods, the RCA near-field feed<sup>11</sup> is the simplest, since it requires no change in the subreflector position. The main disadvantages of this feed are its large size, relative proximity to the subreflector, and possible frequency-sensitive interaction with the subreflector.

If the subreflector can be defocused over a distance of several wavelengths, efficient operation with a wide range of feed horn sizes is possible. The horn and subreflector must be properly positioned for optimum performance. The main requirements on the feed are that it be

operated approximately in its far-field region, and that spillover losses be low. In practice, this would involve the use of relatively small horns. The disadvantages of this system are the far-out location of the feed and the rather large axial displacement of the subreflector.

The efficient operation with the defocused subreflector is due to the fact that the subreflector shape is not critical. Compensatory defocusing can render a wide range of subreflector shapes usable with reasonable efficiency in a given Cassegrainian system. Use of a three-reflector system was shown to result in low secondary gain. This is a direct result of the low beam efficiency of the small dish. Since the phase and amplitude patterns of the small dish are satisfactory when the primary feed is focused for the near field, any improvement in secondary efficiency must come from a corresponding improvement in the beam efficiency of the small dish. Substantial improvement in this area seems unlikely, due to the spillover loss around the small dish, aperture blockage by the primary feed, and the relatively small size of the dish in wavelengths. The experimental results indicate that the size of the small dish was a major cause of the low efficiency. Nevertheless, it would be desirable to determine the maximum attainable beam efficiency of a small dish at a more convenient test frequency than that used in this investigation.

If high efficiency is not required, the three-reflector system is a good choice due to its compactness and good patterns. Little or no subreflector defocusing is necessary. If high efficiency is desired with a focused-aperture feed located near the vertex of the main dish, a lens-corrected horn should be investigated. Another potentially efficient but not compact feed is the horn reflector, provided the proper phase distribution is produced across its aperture.

Further work should include a theoretical and experimental investigation of the amplitude and phase of the field at the feed location  $P_1$  (Fig. 1) as a function of subreflector position. This information would make possible the optimum design of the phase and amplitude distributions at the feed aperture. The effects of shaped, nonoptical subreflectors<sup>14</sup> may also be determined in this manner.

#### ACKNOWLEDGMENTS

The author wishes to thank Dr. J. Ruzic and Dr. K. J. Keeling for helpful discussions. He is indebted to W. D. Fitzgerald for a critical reading of the manuscript. A. Sotiropoulos contributed his design of the Clavin feed and E. F. Pehrine provided able assistance in the experimental work.

APPENDIX A  
LOW FREQUENCY LIMIT OF CASSEGRAINIAN GEOMETRY

A conventional Cassegrainian antenna usually has its subreflector in the far field of the feed. This condition is specified by

$$R \geq \frac{2A^2}{\lambda}$$

where  $R$  is the distance of the subreflector from the feed and  $A$  is the feed aperture dimension. As long as this condition is satisfied, the feed will appear as a point source, regardless of its actual size. The feed is normally adjusted to provide a subreflector edge illumination taper of about 10 dB. Using the diagram of Fig. 1, this can be written as

$$W_{10} = 2\gamma$$

where  $W_{10}$  is the full 10-dB width of the feed radiation pattern. For an average, tapered, feed aperture distribution the diffraction formula of Sec. I-A can be rewritten to give

$$W_{10} \approx \frac{2.1\lambda}{A}$$

Also, for small  $\gamma$ ,

$$2\gamma \approx \frac{d}{R}$$

where  $R$  is taken equal to  $(f_1 + f_2)$ , and  $d$  is the subreflector diameter.

Combining the preceding three equations, we have

$$R = \frac{Ad}{2.1\lambda}$$

This expression is based only on the illumination requirement and the Cassegrainian geometry.

Combining the expression for  $R$  based on the far-field requirement and on the illumination requirement, we have

$$\frac{2A^2}{\lambda} = R = \frac{Ad}{2.1\lambda}$$

from which follows the first important Cassegrainian restriction:

$$A \leq \frac{d}{4.2}$$

Also, from

$$R = \frac{Ad}{2.1\lambda} \leq \frac{(d/4.2)d}{2.1\lambda}$$

we obtain

$$R \leq \frac{0.11 d^2}{\lambda}$$

These final expressions for  $A$  and  $R$  satisfy both the illumination and the far-field conditions.

The magnification factor of a Cassegrainian geometry is given by

$$M = \frac{\tan(\Theta/2)}{\tan(\gamma/2)} \approx \frac{\tan(\Theta/2)}{\gamma/2}$$

Using the well-known angular relation for a parabolic reflector,  $\tan(\Theta/2) = 1/[4(F/D)]$ , the magnification can be simplified to

$$M \approx \frac{1}{2\gamma(F/D)} \approx \left(\frac{R}{F}\right) \left(\frac{D}{d}\right)$$

With the above value for  $R$ , the second Cassegrainian restriction is obtained:

$$M \leq \frac{0.11}{(F/D)} \left(\frac{d}{\lambda}\right)$$

The low frequency "limit" can be written as

$$\lambda_L \leq \frac{0.11}{(F/D)} \left(\frac{d}{M}\right)$$

Since the far-field and illumination conditions used to derive the above expressions are somewhat flexible, the restrictions on  $A$ ,  $M$ , and  $\lambda_L$  are also moderately flexible. In addition, the approximations used tend to reduce the accuracy of the formulas for smaller values of  $M$ . Gross violation of the restrictions, however, will produce improper illumination and result in a serious deterioration in system performance.

The preceding discussion applies to typical horn feeds which do not have a phase error and cannot be focused. If the feed aperture can be phased (focused), the far-field condition considered above is not applicable. Instead, the "far field" of the focused aperture exists only at the distance for which it is focused. Efficient system operation in such a case is therefore possible.

## APPENDIX B

### BEAM EFFICIENCY

If the measured radiation patterns and gain of an antenna are available, the power actually radiated can be calculated. This is quite easy to do in the case of typical antennas radiating a well-defined main beam. The amount of power radiated by the main beam within any included angle  $2\Theta_1$  is given by

$$P_{\Theta_1} = \int_0^{2\pi} \int_0^{\Theta_1} P(\Theta, \varphi) \sin \Theta \, d\Theta \, d\varphi$$

where

$$P(\Theta, \varphi) = \frac{P_t G(\Theta, \varphi)}{4\pi}$$

$P_t$  = total power radiated

$G(\Theta, \varphi)$  = gain function of antenna .

In the case of relatively narrow beams of circular cross section, the above expression simplifies to

$$P_{\Theta_1} \approx \frac{P_t}{2} \int_0^{\Theta_1} G(\Theta) \sin \Theta \, d\Theta$$

where  $\sin \Theta \approx \Theta$  was assumed. The beam efficiency  $\eta_b$  is defined as the relative amount of power in the beam to a specified width:

$$\eta_b = \frac{P_{\Theta_1}}{P_t} .$$

The main beam of most horn and dish antennas has a typical shape that can be approximated by several simple functions.<sup>15</sup> One of the more accurate of these is given by

$$G(\Theta) = G_o \left( \frac{\sin N\Theta}{N\Theta} \right)^2$$

where  $G_o$  is the gain and  $N$  is determined by the width of the beam. In practice, a better fit for a measured pattern is obtained by using the full 10-dB width  $W_{10}$ , rather than the full half-power width  $W_3$ . Thus, the value of  $N$  is found from the condition

$$\frac{G(\Theta_{10})}{G_o} = 0.1$$

where  $\Theta_{10} = W_{10}/2$ . Using the properties of the  $\sin x/x$  function, the following relations are derived:

$$N = \frac{2.32}{\Theta_{10}} = \frac{4.64}{W_{10}} \quad (\Theta_{10}, W_{10} \text{ in radians})$$

or

$$N = \frac{266}{W_{10}} \quad (W_{10} \text{ in degrees}) .$$

If only the 3-dB width is available, the 10-dB width can be found from the following equation:

$$W_{10} = 1.67 W_3$$

Once  $N$  and  $G_o$  are determined from the measured data, the beam efficiency  $\eta_b$  can be calculated:

$$\begin{aligned} \eta_b &= \frac{P_{\Theta_1}}{P_t} = \frac{G_o}{2(N)^2} \int_0^{N\Theta_1} \frac{\sin^2(N\Theta)}{(N\Theta)} d(N\Theta) \\ &= \frac{G_o}{(2N)^2} \text{Cin}(2N\Theta_1) \\ &= 3.535 \times 10^{-6} G_o (W_{10})^2 \text{Cin}\left(9.28 \frac{\Theta_1}{W_{10}}\right) \end{aligned}$$

where  $W_{10}$  is in degrees and the function  $\text{Cin}(x)$  is tabulated in Kraus.<sup>16</sup> For the 10-dB width, the beam efficiency is given by

$$\eta_b = 8.16 \times 10^{-6} G_o (W_{10})^2$$

For example, a typical dish has a 10-dB beamwidth given by the empirical formula

$$W_{10} = \frac{117\lambda}{D}$$

where  $\lambda$  is the wavelength and  $D$  is the diameter. A typical gain representing 55 percent aperture efficiency is similarly given by the empirical formula

$$G_o = \frac{75,300}{(W_{10})^2}$$

From these formulas, the 10-dB beam efficiency is found to be

$$\eta_b = 8.16 \times 10^{-6} (75,300) = 0.614$$

Thus, a typical dish has approximately 61 percent of the total radiated power in the upper 10-dB portion of the main beam.

In a similar fashion, the beam efficiency of the entire main beam down to the nulls is given by

$$\eta_b = 8.16 \times 10^{-6} G_o (W_{10})^2$$

This is a bit on the low side, since the  $\sin(N\Theta)/N\Theta$  function is too narrow at the nulls when fitted to typical patterns at the 10-dB level. For the typical dish above, the beam efficiency for the entire main beam is

$$\eta_b = 8.16 \times 10^{-6} (75,300) = 0.647$$

Thus, about two-thirds of the power radiated by a typical dish is contained in the main lobe.

## REFERENCES

1. R. C. Hansen, Microwave Scanning Antennas, Vol. I (Academic Press, New York, 1964), pp. 40 and 90.
2. D. K. Cheng and S. T. Moseley, "On-Axis Defocus Characteristics of the Paraboloidal Reflector," Trans. IRE Antennas Propag. AP-3, 214 (1955).
3. P. D. Potter, "Unique Feed System Improves Space Antennas," Electronics 35, 36-40 (1962).
4. W. V. T. Rusch, "Scattering from a Hyperboloidal Reflector in a Cassegrainian Feed System," Trans. IEEE Antennas Propag. AP-11, 414 (1963).
5. P. D. Potter, "The Design of a Very High Power, Very Low Noise Cassegrainian Feed System for a Planetary Radar," Technical Report 32-653, Jet Propulsion Laboratory (24 August 1964).
6. A. Sotiropoulos, "Radiometric Feed for Haystack," Technical Note 1965-23, Lincoln Laboratory, M.I.T. (15 June 1965).
7. D. C. Hogg and R. A. Semplak, "An Experimental Study of Near-Field Cassegrainian Antennas," Bell System Tech. J. 43, 2677 (1964).
8. K. J. Keeping, "A Wideband Antenna Having Axially Symmetrical Patterns, High Gain, and Low Sidelobes for All Polarizations," Group Report 46G-0008, Lincoln Laboratory, M.I.T. (30 November 1960), DDC 248360.
9. H. Ujiie, T. Yoneyama, and S. Nishida, "A Consideration of the Phase Center of Aperture Antennas," Trans. IEEE Antennas Propag. AP-15, 478 (1967).
10. W. T. Slayton, "Design and Calibration of Microwave Antenna Gain Standards," Report 4433, Naval Research Laboratory (9 November 1954), p. 9. Also Electronics 28, 150 (1955).
11. C. E. Profera, Jr. and L. H. Yorinks, "An Improved Cassegrainian Monopulse Feed System," 17th Annual Symposium, USAF Antenna Research and Development Program, University of Illinois (14-16 November 1967).
12. A. Chlavin, "A New Antenna Feed Having Equal E- and H-Plane Patterns," Trans. IRE Antennas Propag. AP-2, 113 (1954).
13. D. K. Cheng, "On the Simulation of Fraunhofer Radiation Patterns in the Fresnel Region," Trans. IRE Antennas Propag. AP-5, 399 (1957).
14. P. D. Potter, "Application of Spherical Wave Theory to Cassegrainian-Fed Paraboloids," Trans. IEEE Antennas Propag. AP-15, 727 (1967).
15. H. C. Ko, "On the Determination of the Disk Temperature and the Flux Density of a Radio Source Using High-Gain Antennas," Trans. IRE Antennas Propag. AP-9, 500 (1961).
16. J. D. Kraus, Antennas (McGraw-Hill, New York, 1950), p. 535.

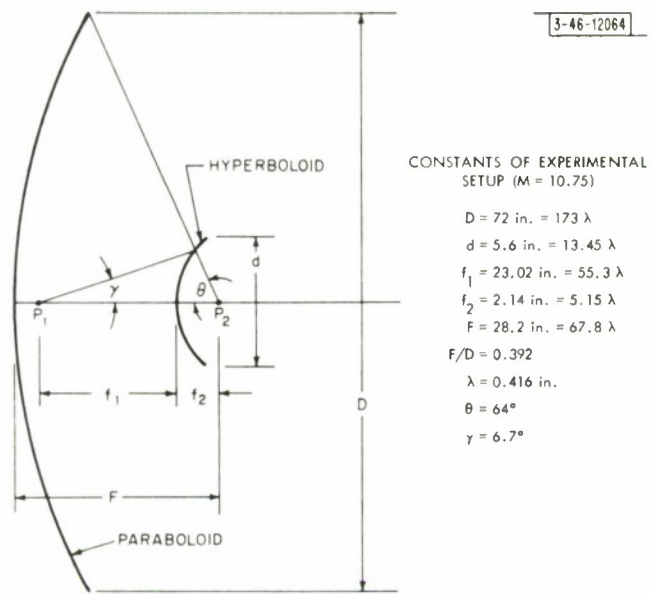


Fig. 1. Cassegrainian geometry.

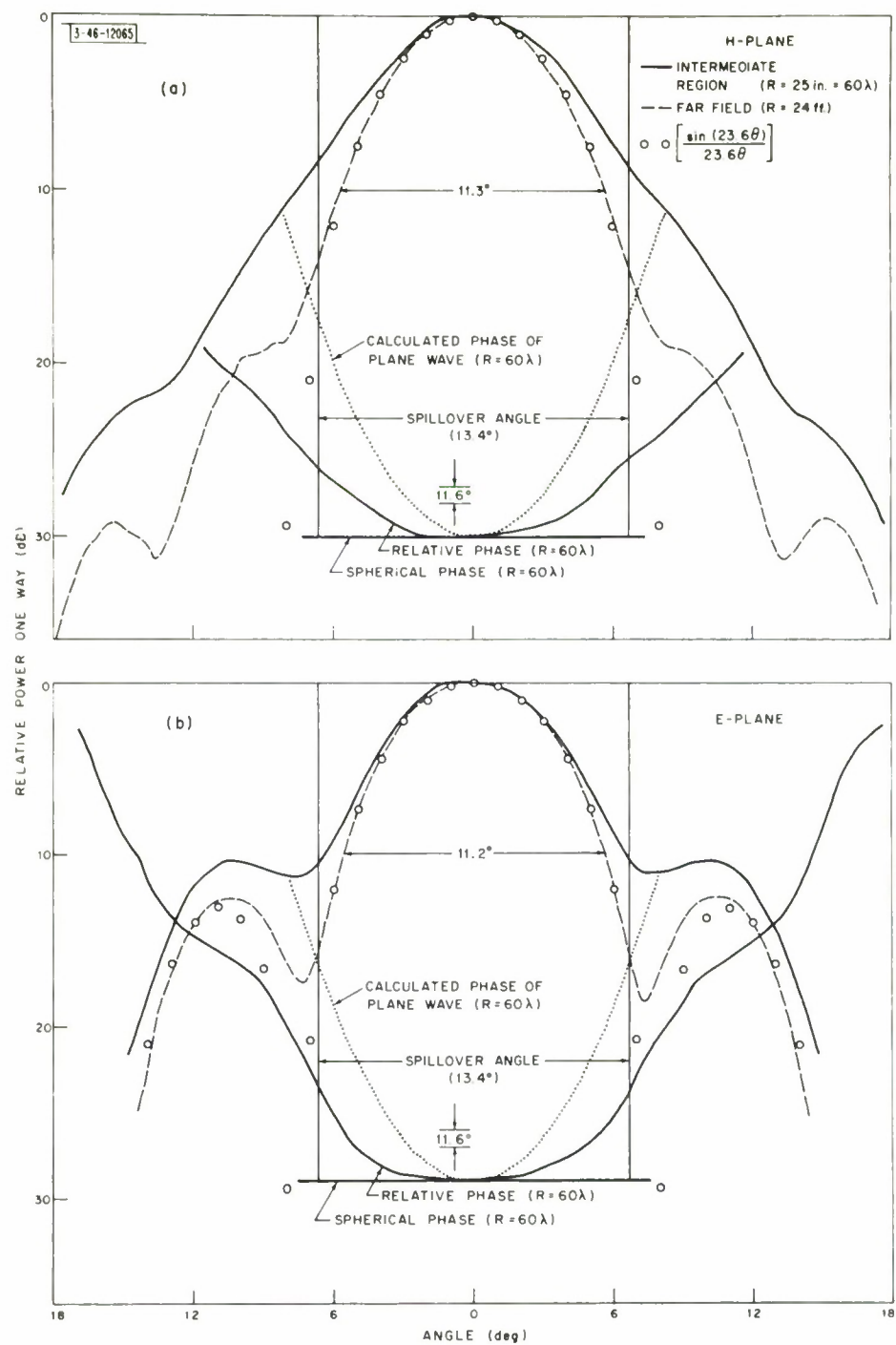


Fig. 2. Primary amplitude and phase patterns of large horn ( $7.65 \times 10.68 \lambda$ ).

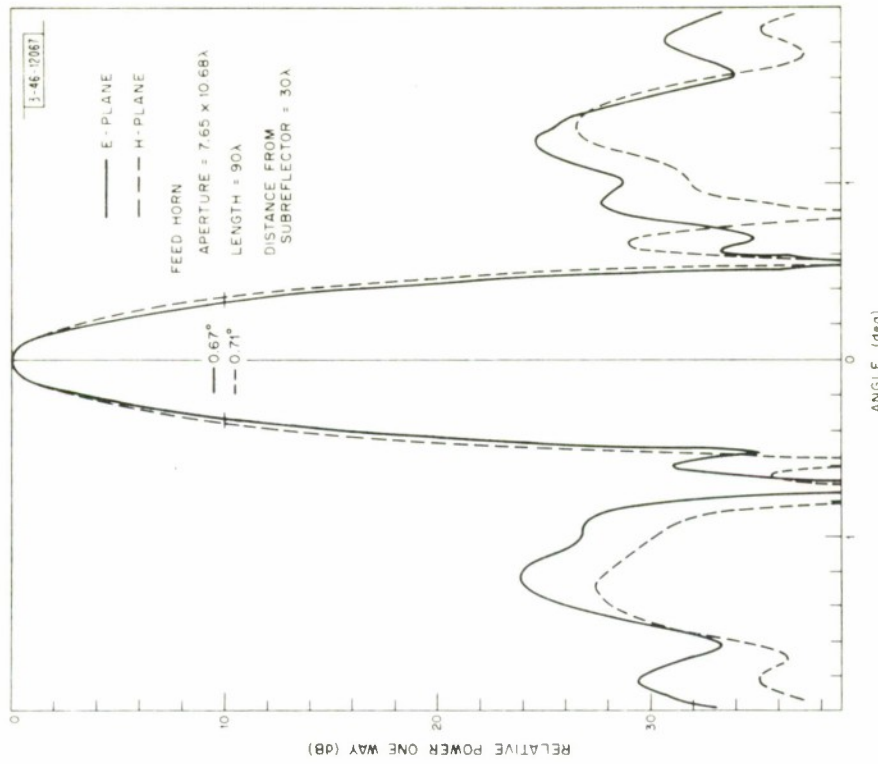


Fig. 4. Secondary patterns of 6-foot Cassegrainian antenna with large horn feed.

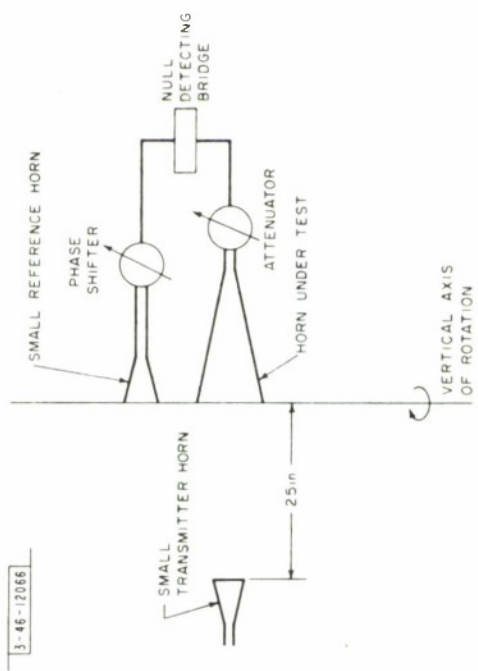


Fig. 3. Phase measurement setup.

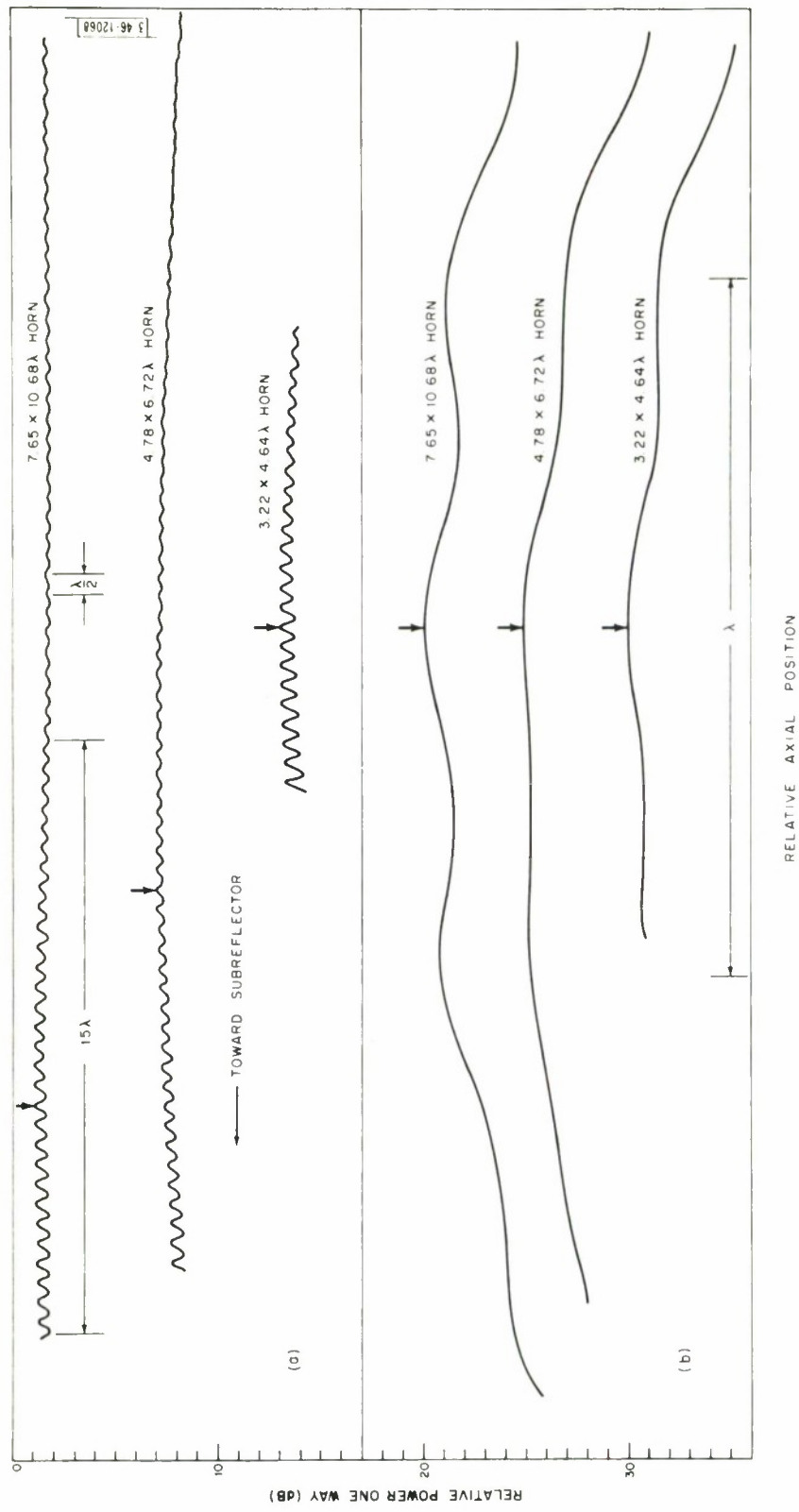


Fig. 5. Secondary gain variation with axial position of (a) feed horn, (b) hyperbolic subreflector.

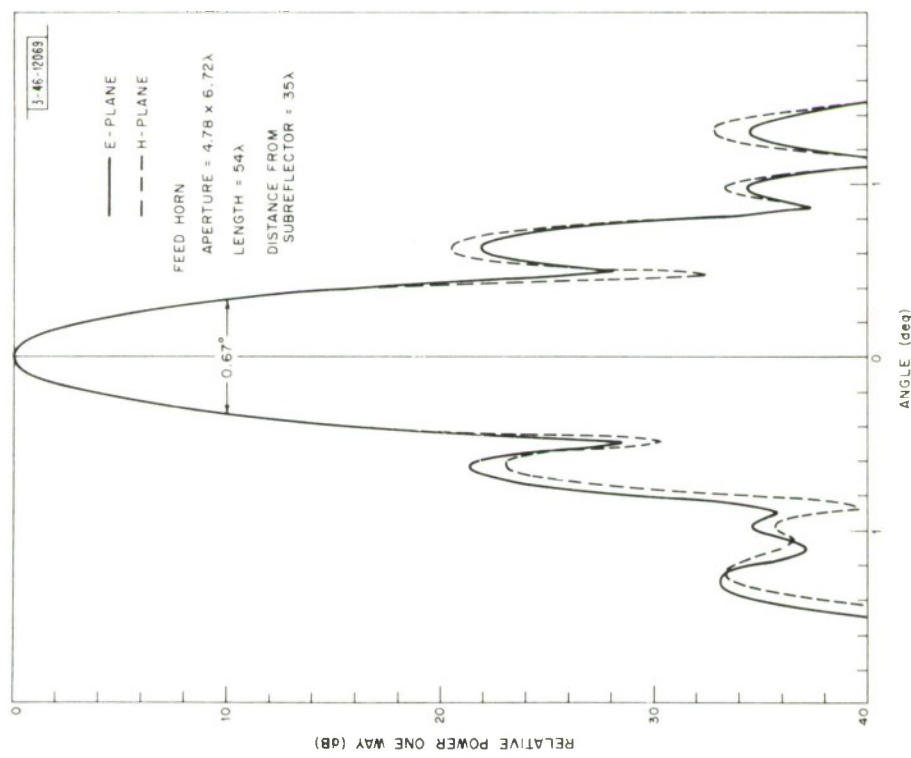
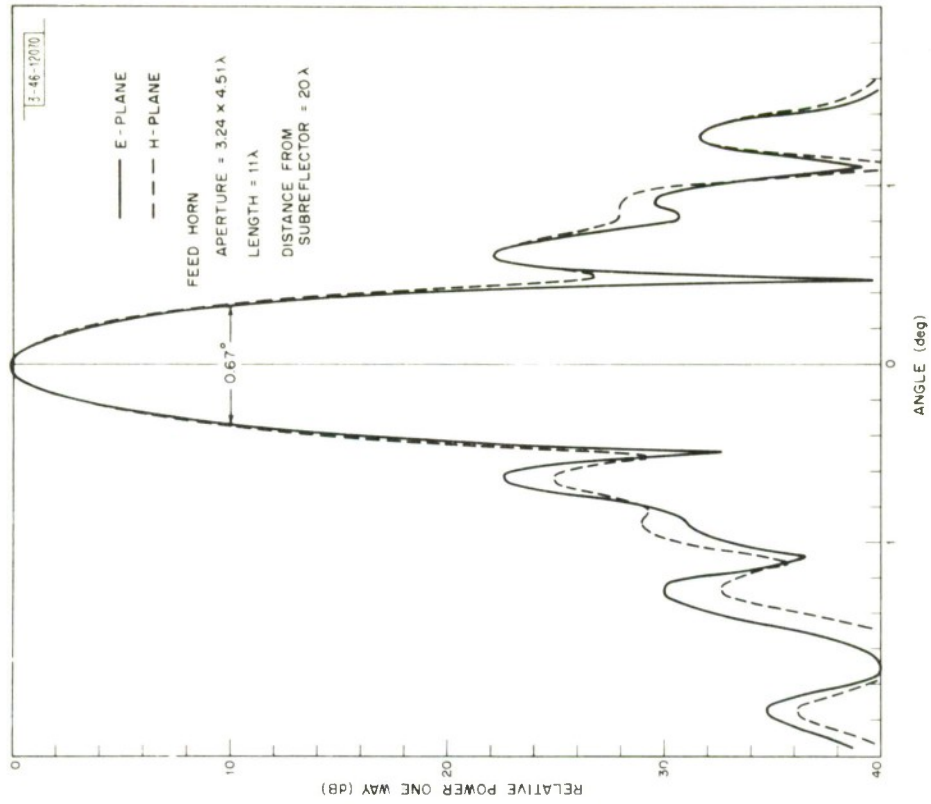


Fig. 6. Secondary patterns of 6-foot Cassegrainian antenna with moderate-size horn feed.

Fig. 7. Secondary patterns of 6-foot Cassegrainian antenna with intermediate-size horn feed.

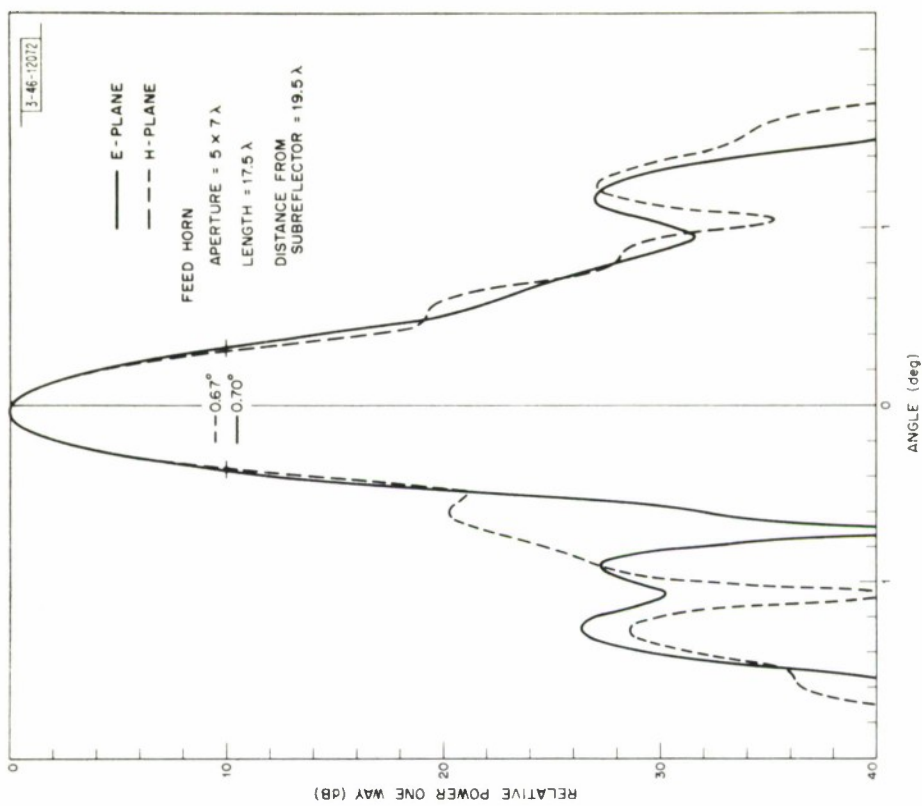


Fig. 8. Secondary patterns of 6-foot Cassegrainian antenna with small horn feed.

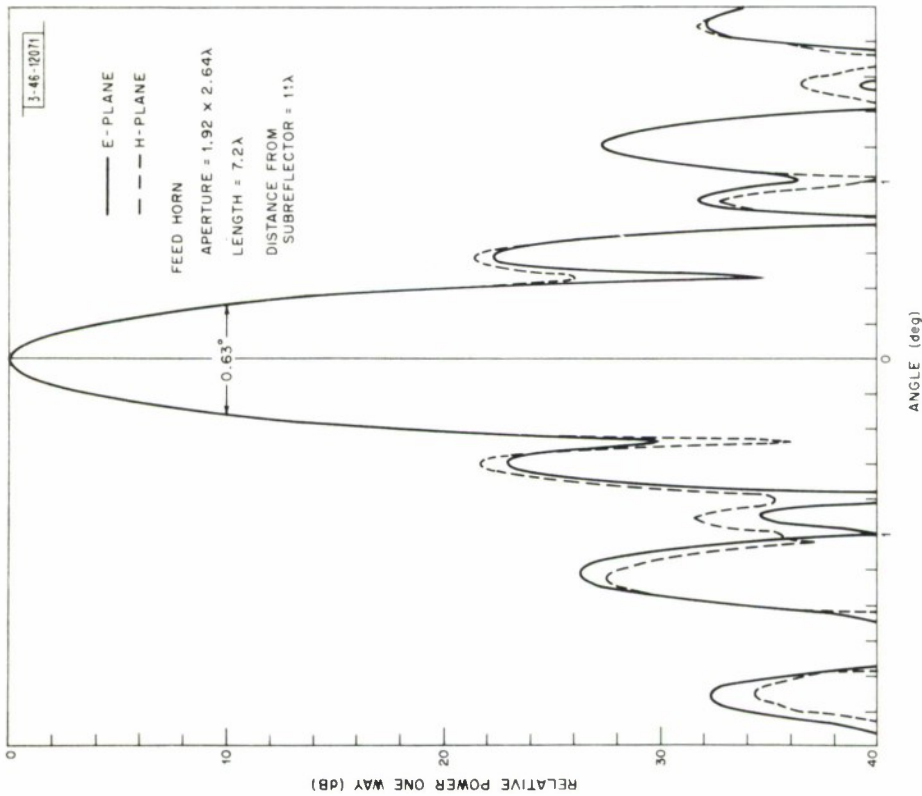


Fig. 9. Secondary patterns of 6-foot Cassegrainian antenna with rectangular horn feed having phase error.

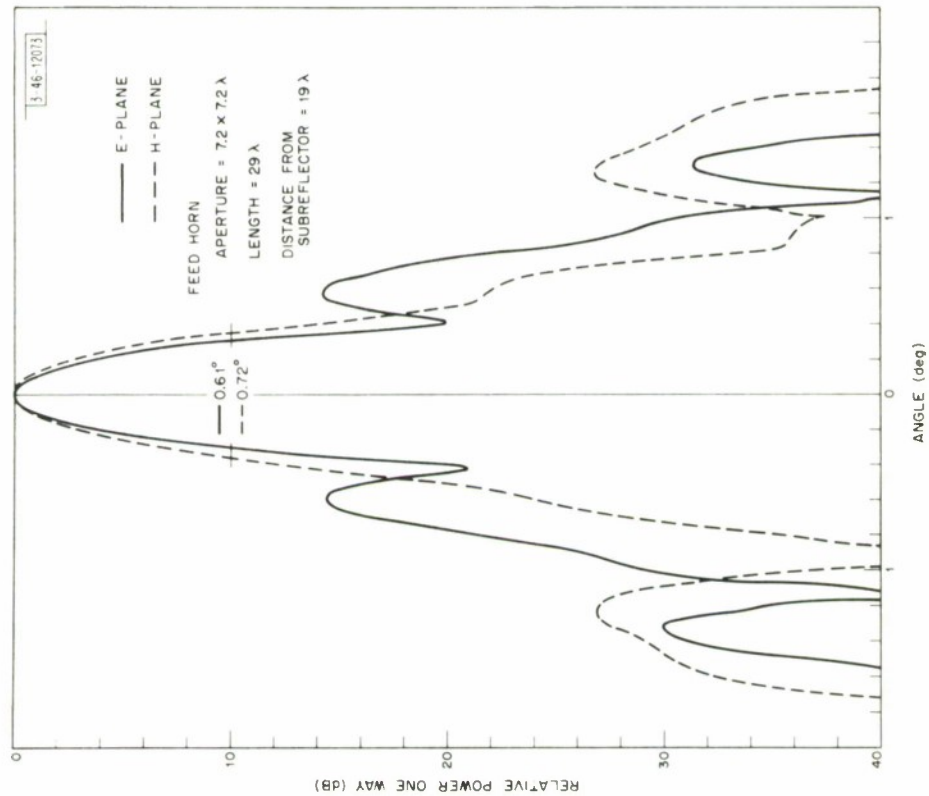
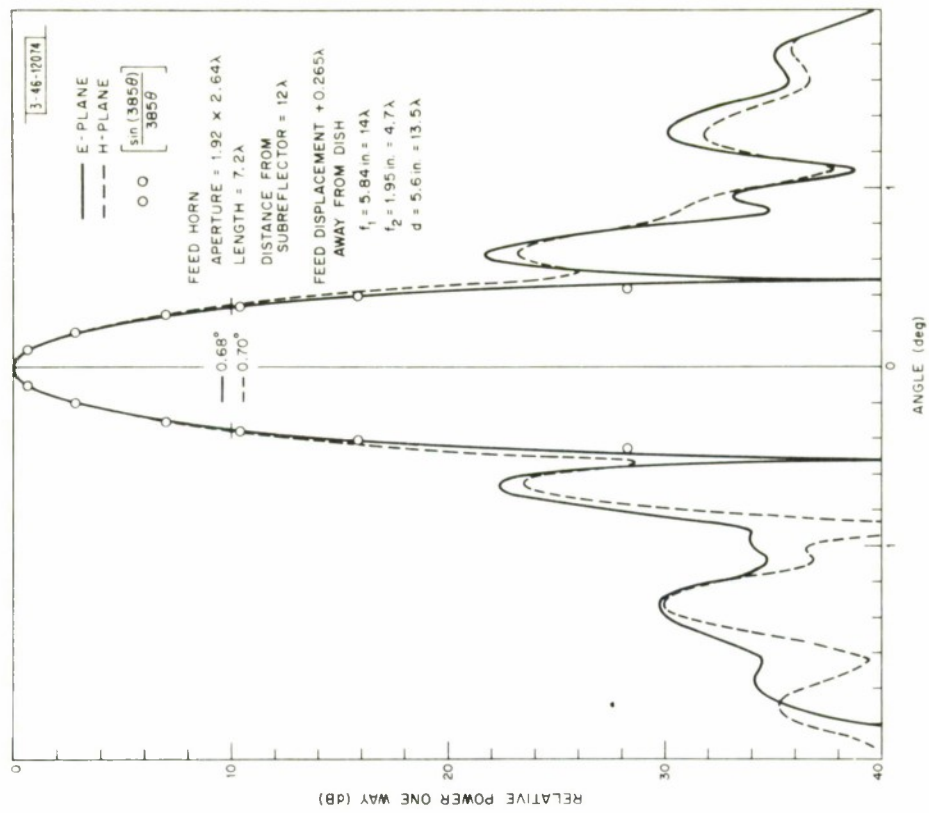


Fig. 10. Secondary patterns of 6-foot Cassegrainian antenna with square horn feed having phase error.

Fig. 11. Secondary patterns of 6-foot Cassegrainian antenna ( $M = 3$ ) with small horn feed.

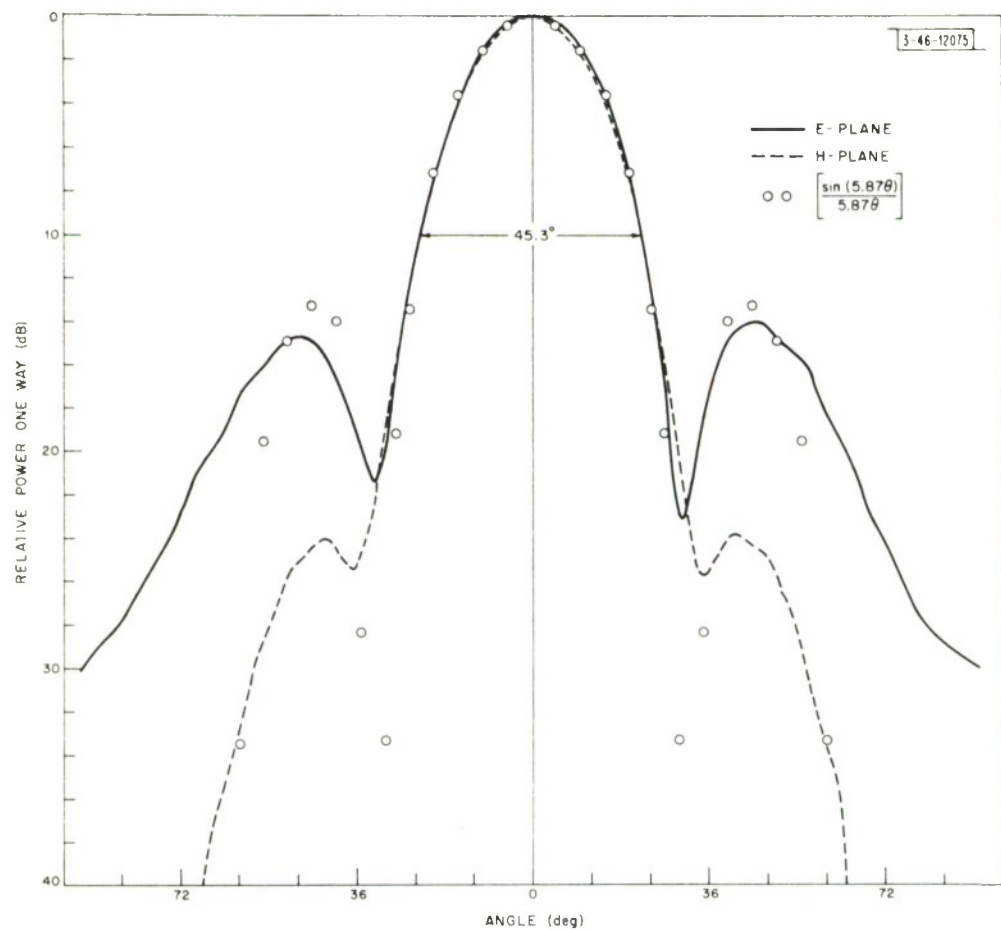


Fig. 12. Primary pattern of small horn ( $1.92 \times 2.64 \lambda$ ).

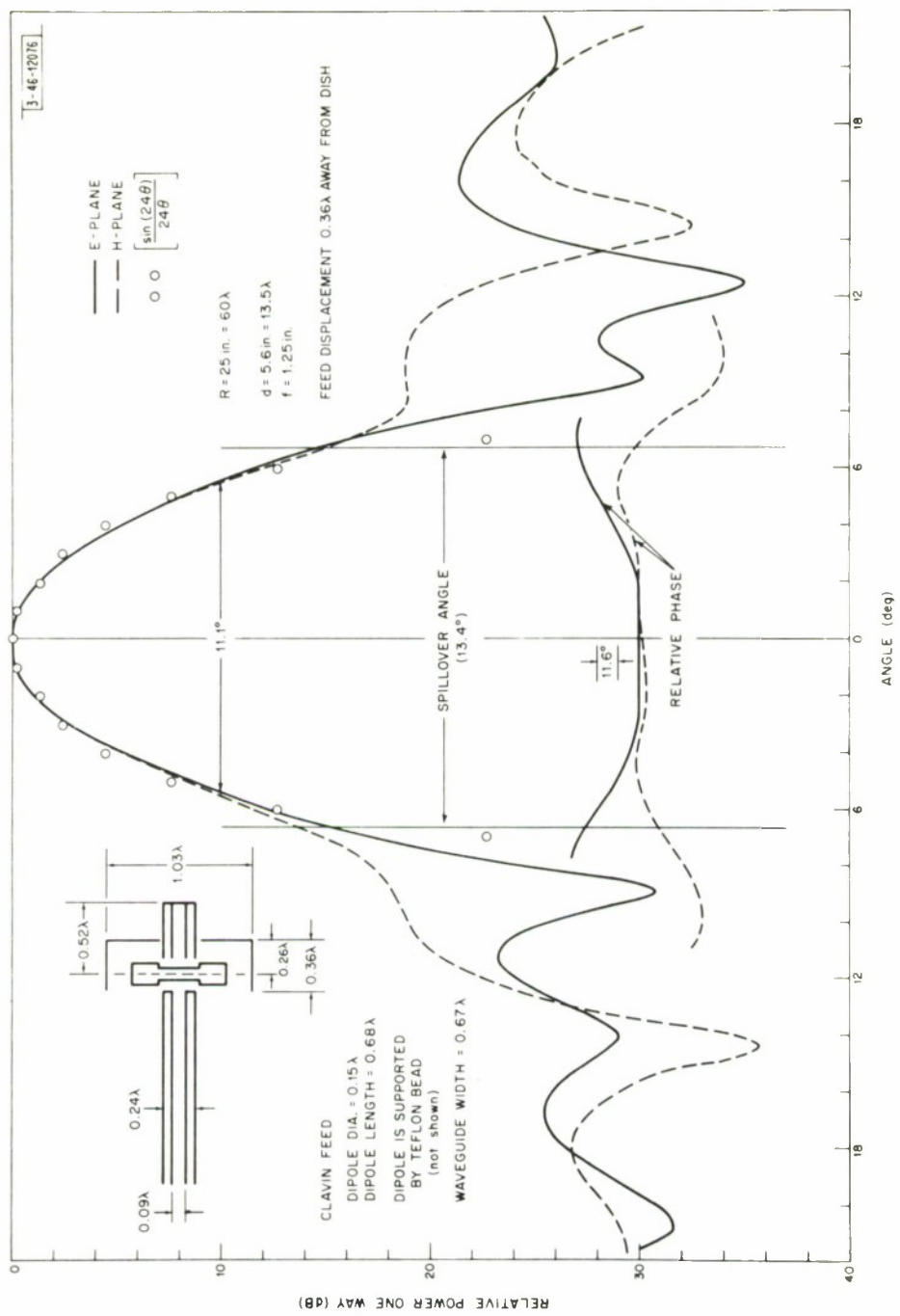


Fig 13. Near-field amplitude and phase patterns of 13.5- $\lambda$  dish with Clavin feed.

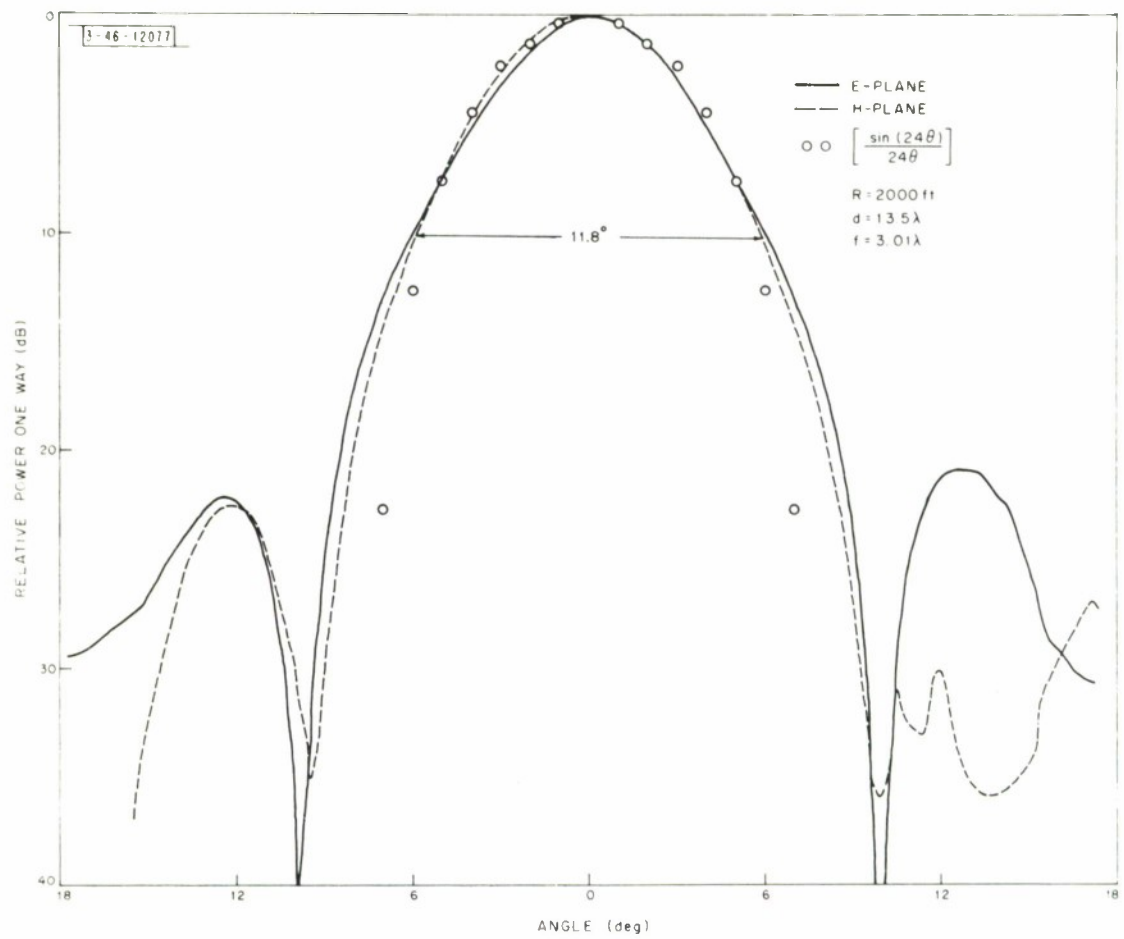


Fig. 14. Far-field radiation patterns of  $13.5\lambda$  dish with Clavin feed.

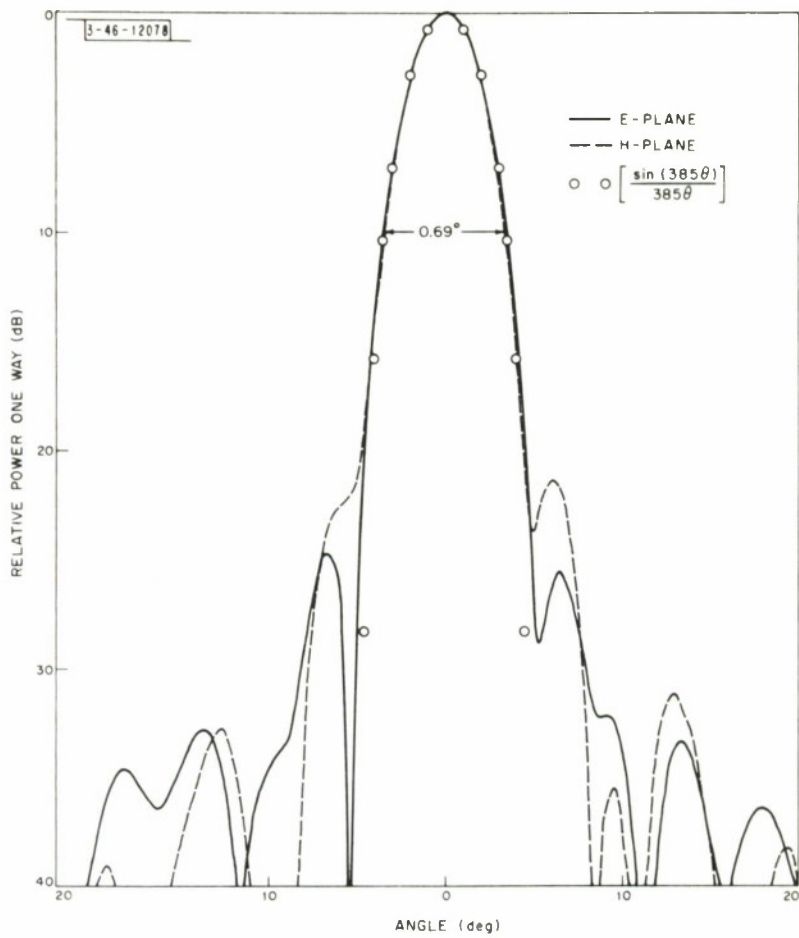


Fig. 15. Patterns of 6-foot Cassegrainian antenna with  $13.5\lambda$  dish and Clavin feed.

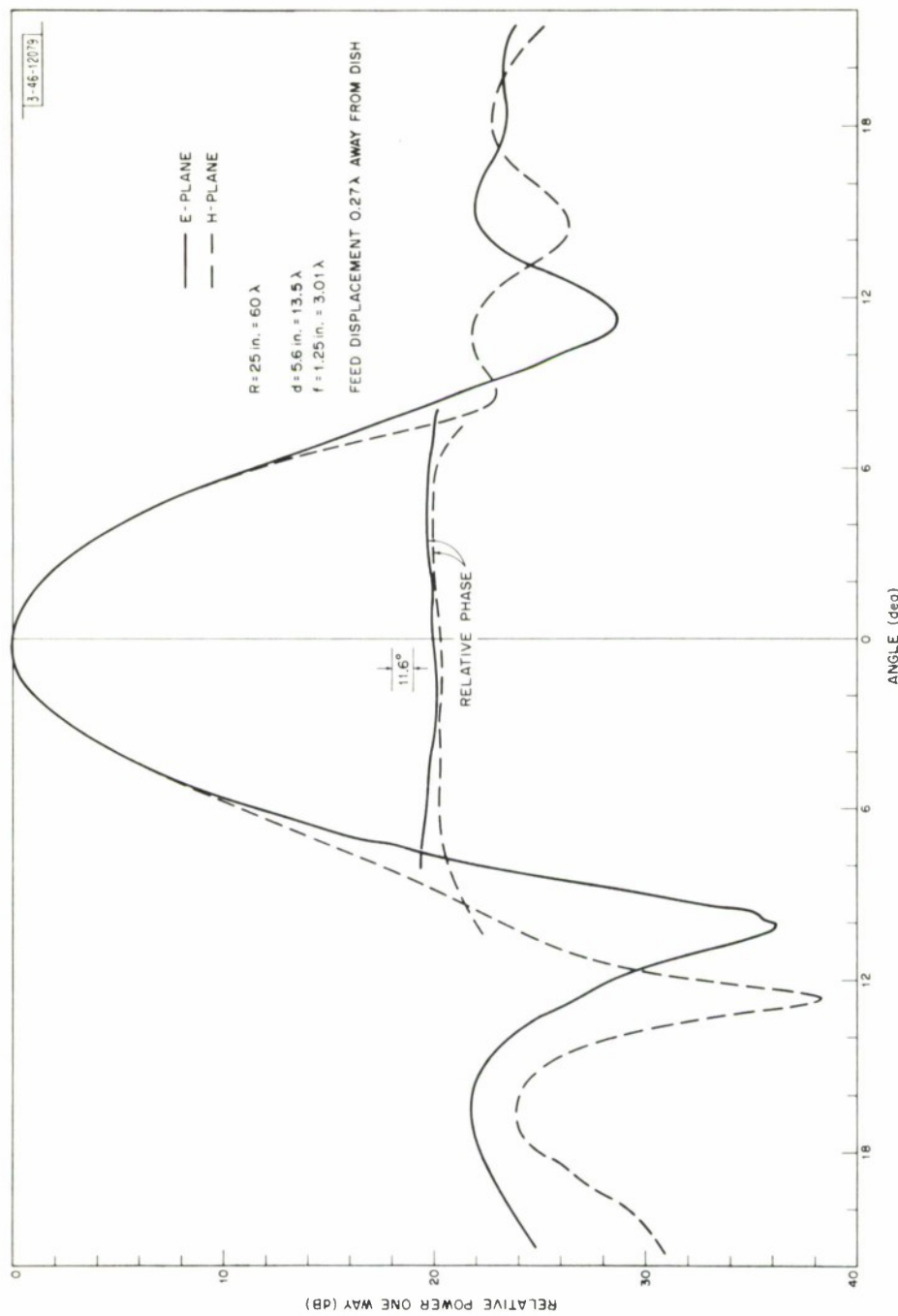


Fig. 16. Near-field radiation patterns of  $13.5\lambda$  dish with circular horn feed.

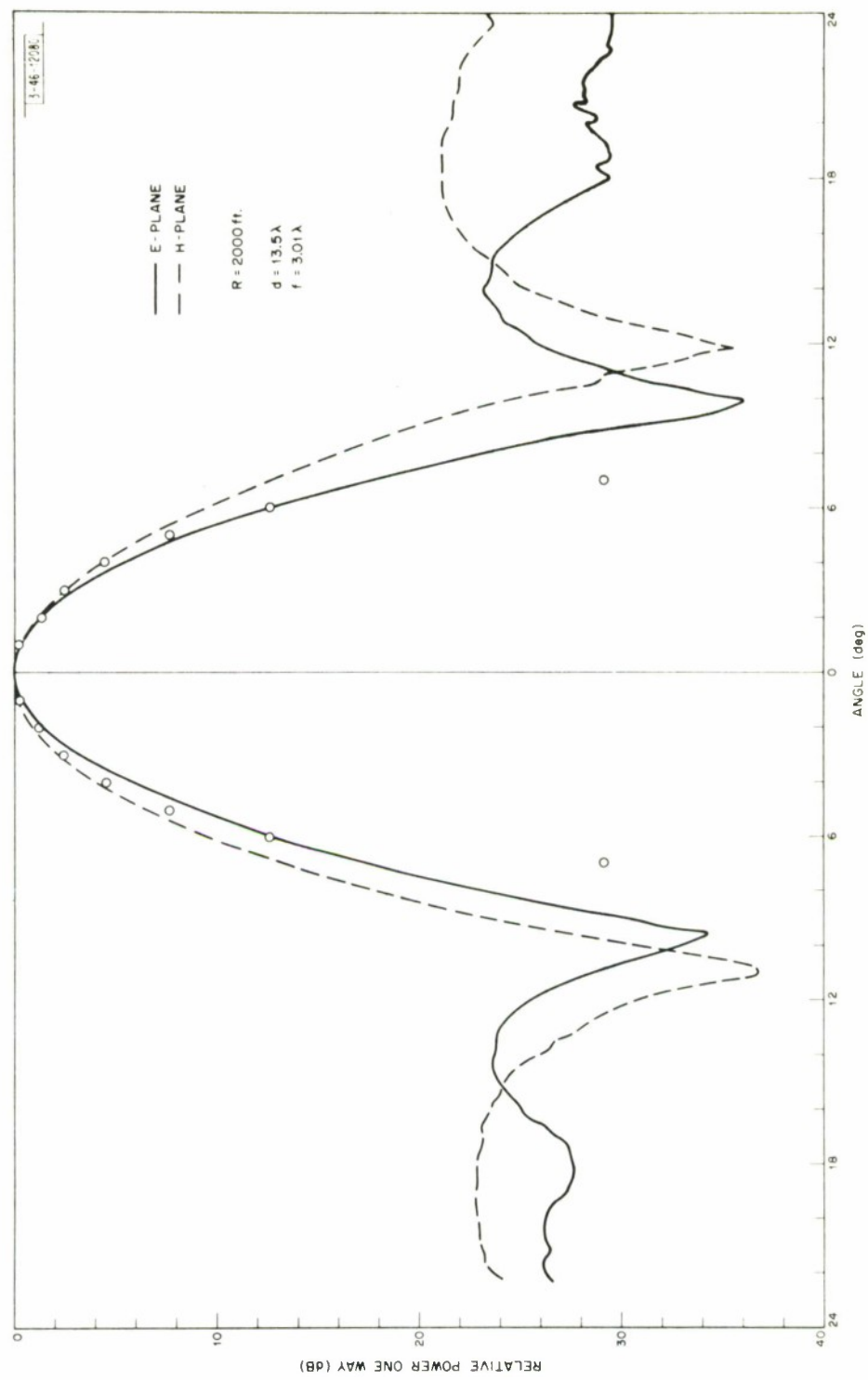


Fig. 17. Far-field radiation patterns of  $13.5\text{-}\lambda$  dish with circular horn feed.

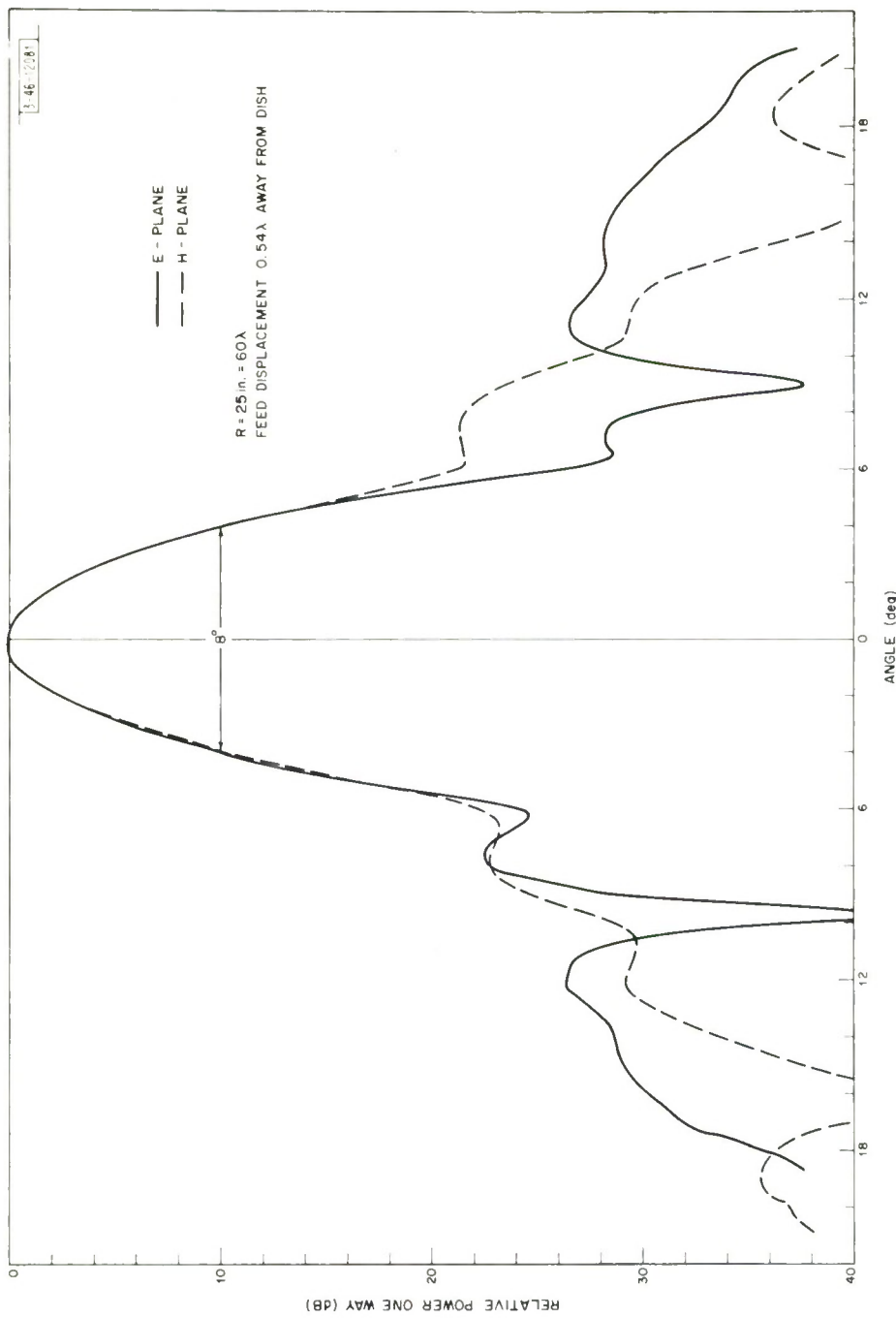


Fig. 18. Near-field patterns of  $19\text{-}\lambda$  dish with Clavin feed.

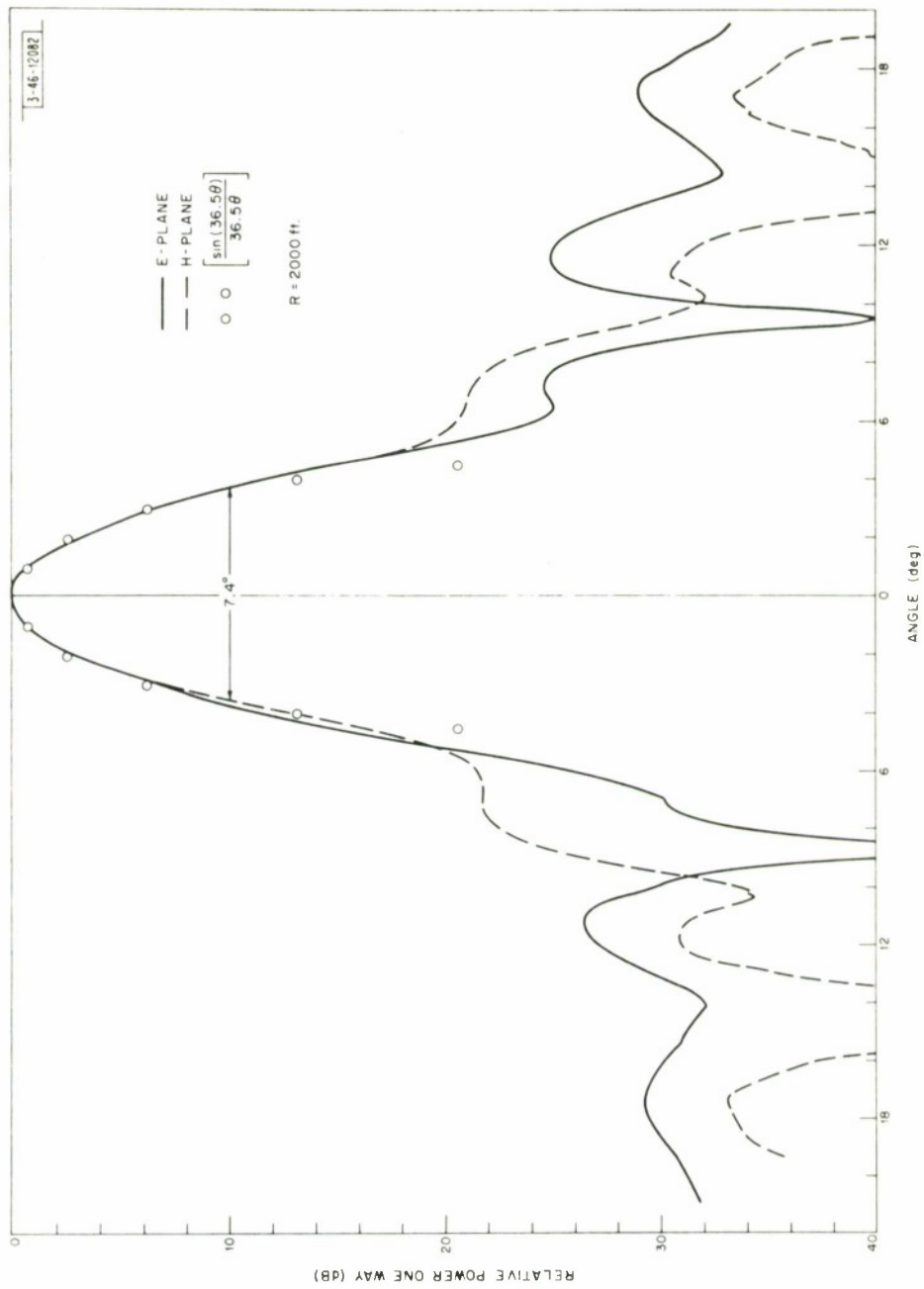


Fig. 19. Far-field patterns of  $19\lambda$  dish with Clavin feed.

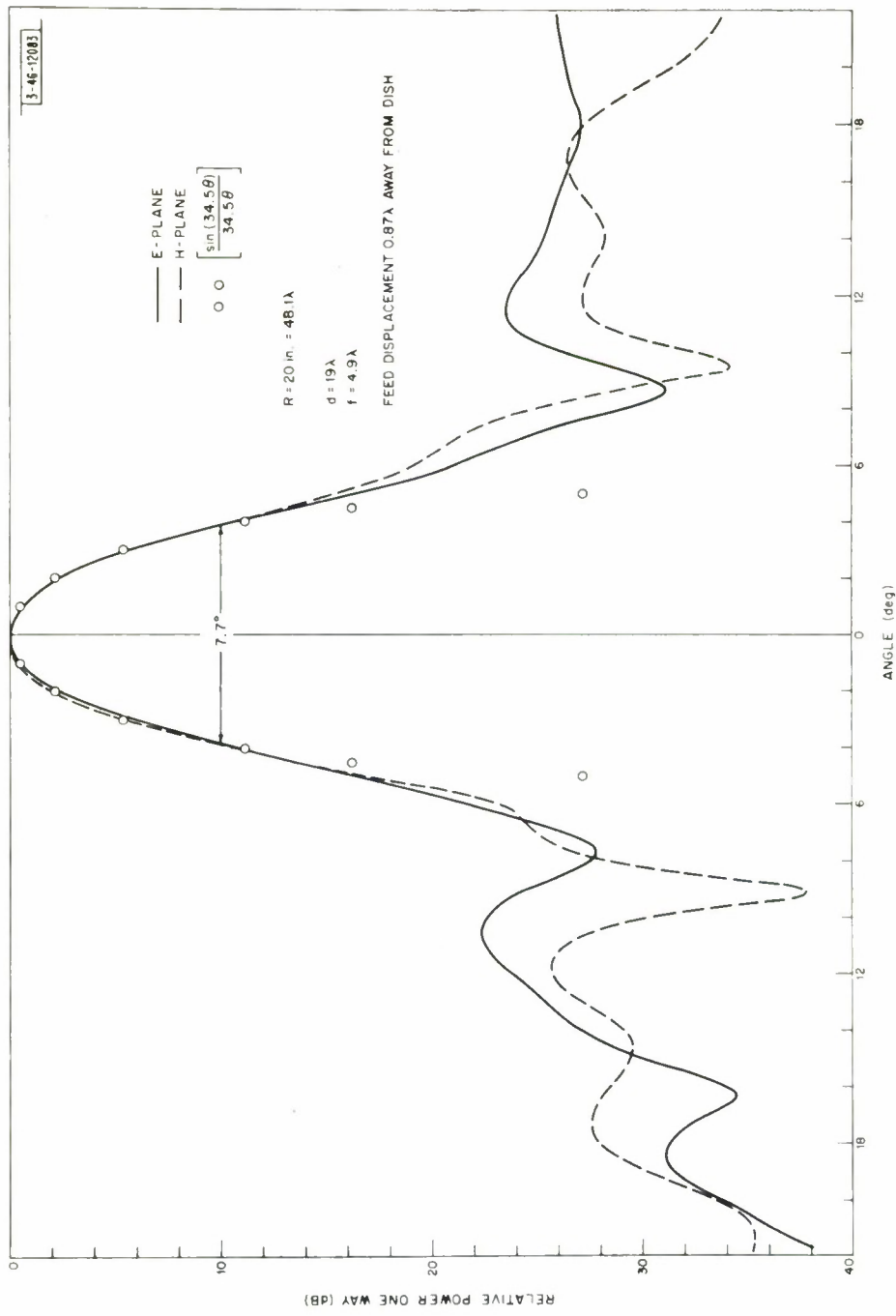


Fig. 20. Near-field patterns of  $19\lambda$  dish with circular feed horn.

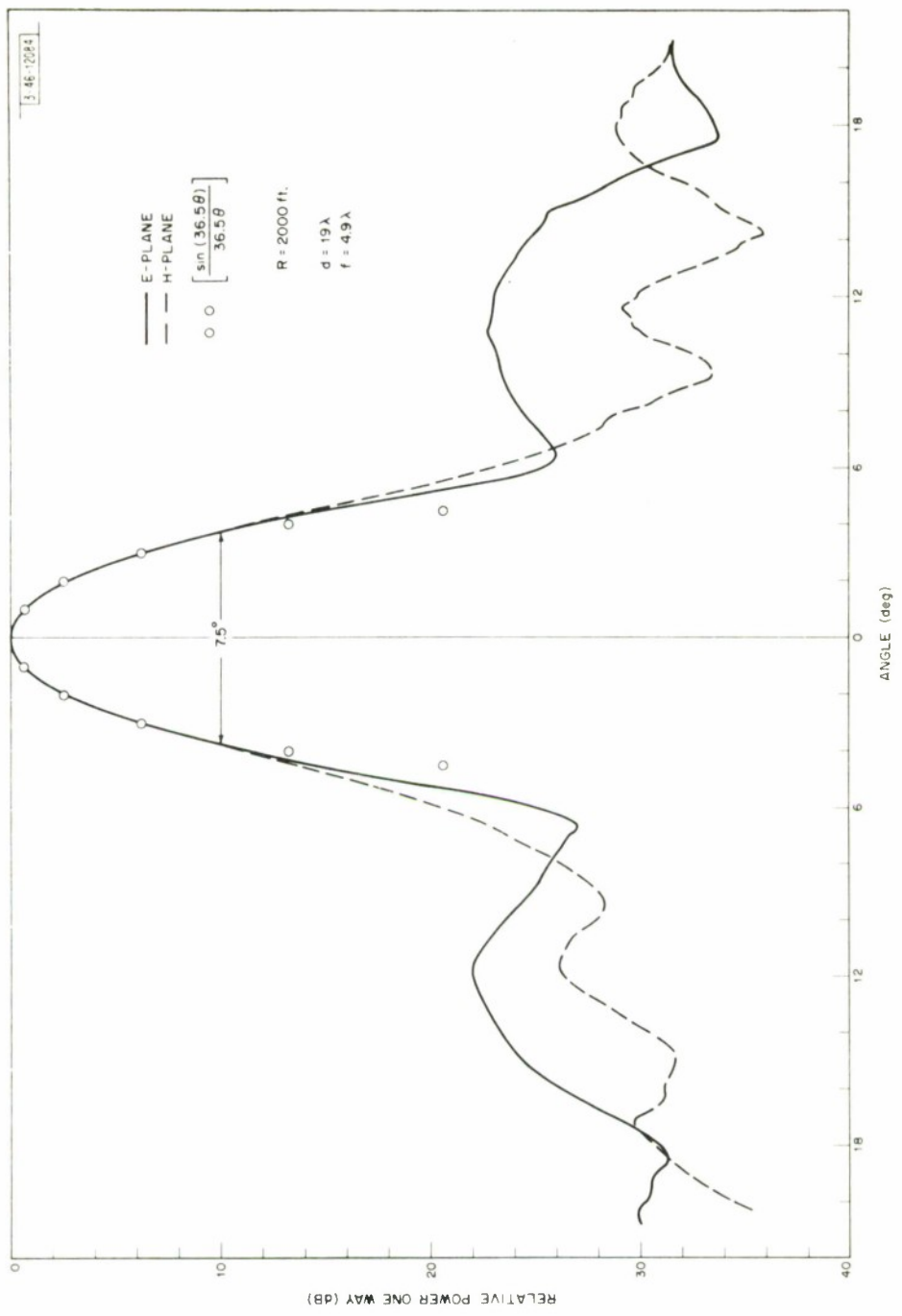


Fig. 21. Far-field patterns of  $19\lambda$  dish with circular feed horn.

DOCUMENT CONTROL DATA - R&D

(Security classification of title, body of abstract and indexing annotation must be entered when the overall report is classified)

1. ORIGINATING ACTIVITY (Corporate author) Lincoln Laboratory, M.I.T.	2a. REPORT SECURITY CLASSIFICATION Unclassified
	2b. GROUP None

3. REPORT TITLE

Experimental Study of the Low Frequency Operation of a Cassegrainian Antenna

4. DESCRIPTIVE NOTES (Type of report and inclusive dates)

Technical Note

5. AUTHOR(S) (Last name, first name, initial)

Sheftman, Franklin I.

6. REPORT DATE 10 December 1968	7a. TOTAL NO. OF PAGES 44	7b. NO. OF REFS 16
------------------------------------	------------------------------	-----------------------

8a. CONTRACT OR GRANT NO.  
AF 19 (628)-5167

9a. ORIGINATOR'S REPORT NUMBER(S)

Technical Note 1968-38

b. PROJECT NO.

649L

9b. OTHER REPORT NO(S) (Any other numbers that may be assigned this report)

ESD-TR-68-360

c.

d.

10. AVAILABILITY/LIMITATION NOTICES

This document has been approved for public release and sale; its distribution is unlimited.

11. SUPPLEMENTARY NOTES None	12. SPONSORING MILITARY ACTIVITY Air Force Systems Command, USAF
---------------------------------	---

13. ABSTRACT

The maximum allowable magnification factor of a conventional Cassegrainian antenna is shown to depend on the subreflector size in terms of wavelength. Use of excessively high magnification leads to inefficient operation, unless special precautions are taken. It is demonstrated experimentally that, for a given subreflector, satisfactory results can be obtained with a variety of feed horn sizes and locations, provided the subreflector can be defocused a distance of up to a few wavelengths. It is further shown that the subreflector shape is not critical if sufficient room is available for compensatory defocusing. Efficient operation is also possible without subreflector defocusing in a near-field configuration involving a large feed horn placed close to a subreflector having high magnification. The three-reflector system, which uses a small dish as the feed aperture, can be operated with little or no subreflector defocusing, but the system has low efficiency due to the low efficiency of the small dish.

14. KEY WORDS

antennas  
Cassegrainian antennas  
subreflectors

hyperbolic subreflectors  
feed horns  
subreflector defocusing